Skin layer of diffusive media

Th. M. Nieuwenhuizen

Van der Waals–Zeeman Laboratorium, Valckenierstraat 65, 1018 XE Amsterdam, The Netherlands

J. M. Luck

Service de Physique Théorique, Centre d'Études de Saclay, 91191 Gif-sur-Yvette CEDEX, France

(Received 9 November 1992)

The transport of radiation in the bulk of multiply scattering media is well understood within the diffusion approximation. Such a description does not hold in the *skin layers*, where the transport mechanism crosses over from free propagation to diffusive propagation, or vice versa. In this work, we examine the effects of the skin layers of optically thick slabs on various quantities, including the angularly resolved diffuse reflection and transmission and the shape of the enhanced backscattering cone. This study is based on the ladder approximation to the multiple-scattering expansion. It does not rely on the diffusion approximation and incorporates a systematic treatment of the internal reflections which take place when the random-scattering medium and the outside have two different optical indices, in an arbitrary ratio m. Many exact results are recovered in the absence of internal reflections ($m = 1$). A systematic approach describes accurately the large-index-mismatch regime ($m \to 0$ or ∞), where the improved diffusion approximation is shown to become exact asymptotically. The analytic predictions of the large-index-mismatch approach are compared in a detailed way with numerical results and with the outcomes of previous works.

PACS number(s): 42.25.Gy, 42.25.Bs, 42.25.Fx, 42.25.Md

I. INTRODUCTION

The study of light propagation through turbid media has been an intensive field of research for many decades. It has a wide range of applications, including interstellar clouds, stellar atmospheres, fog, milky liquids, human tissues and brains, etc. Physical experiments concern mostly substances such as solid TiO_2 (a component of white paint), teflon, or suspensions of polystyrene spheres or TiO_2 particles in a fluid.

Many aspects of the transport of light in such media are well described by the so-called radiative-transfer equation [1,2]. This transport equation has been derived long ago by astrophysicists. On scales much larger than the mean free path, it is equivalent to a diffusion equation. The transfer equation can also be obtained by summing the contributions of the dominant scattering processes, i.e., the so-called ladder diagrams, in a systematic multiple-scattering expansion.

The diffusion approximation works very well for transport in the bulk of a multiply scattering medium. Among the physical consequences of diffusion theory, let us mention Ohm's law for the electrical conductance, which is equivalent in the present problem to the $1/L$ decay of the total transmission, where L is the sample thickness. Accurate measurements confirming this behavior quantitatively and a comparison with numerical data have been reported, e.g., in Ref. [3]. Another interesting effect due to diffusion concerns speckle correlations. The memory of a typical speckle pattern is lost when the frequency of light is changed by an amount of order $\Delta\nu \sim D/L^2$, where D is the diffusion coefficient [4,5]. Similarly, in time-resolved transmission experiments, the decay of the transient response to a pulse in transmission exhibits a characteristic time constant of order $\tau \sim L^2/D$ [6,7]. More recently, the validity of diffusion theory has been confirmed in an experiment where a small object (a glass fiber or a pencil lead) was placed in a milky liquid. It was found that the effect of the obstacle on the transmission and reflection patterns can be understood quantitatively within diffusion theory [8].

Near the boundaries of a turbid medium, however, the diffusion approximation breaks down for the simple reason that light undergoes too few scattering events. In the *skin layers*, i.e., when the distance to the boundary is of the order of a few times the mean free path, diffusive transport crosses over to free propagation, or vice versa.

In practical situations, the optical index n_0 of the scattering medium is usually different from the index n_1 of the surrounding medium (air or glass). Let $m = n_0/n_1$ denote the ratio of optical indices. The index mismatch causes reflections at the interface. These internal reflections are known to generate important effects for which *ad hoc* corrections have been made in the interpretation of experiments. It has been proposed [9] to describe these effects within an improved diffusion approximation. Although such an approach yields accurate results, it may require new assumptions, or new parameters to be fitted, whenever a new quantity is calculated. One of the surprising outcomes of the present study will be that the improved diffusion approximation becomes asymptotically exact in the limit of a large index mismatch, i.e., for $m \to 0$ or $m \to \infty$. This commonly used scheme will thus be given a mathematical justification.

More generally, the aim of the present work is to provide a microscopic description of the effects of internal reflections on the diffuse transport of waves through thick slabs. We restrict the analysis to scalar waves. For multiply scattered electromagnetic waves, this is realistic provided one studies quantities that are averaged over the polarizations. We mainly consider isotropic scattering by pointlike scatterers located at uncorrelated random positions. (A consistent treatment of point scatterers in $d = 3$ was given recently in Ref. [27].) Since in low-density systems the only relevant property of the scatterers is their far-field t matrix, the assumption of point scatterers is actually not restrictive. However, realistic dielectric particles do not scatter isotropically. The restriction to isotropic scattering will therefore be relaxed in Sec. II G. Finally, we only consider the regime where the mean free path l is much larger than the wavelength λ. This implies that essentially all scatterers are in the farfield of their neighbors. Even in this idealized situation, internal reflections have effects of order unity and thus overshadow many interference and loop effects. Indeed, the latter are typically of the order λ/l.

In Sec. II, we derive the transport equation in the presence of internal reflections, we relate its solutions to physical quantities concerning diffuse reflection and transmission, and enhanced backscattering, and we discuss some consequences of this general formalism. The analysis will be performed for the case of isotropic scattering. The situation of anisotropic scattering will be discussed briefly in Sec. II G. In Sec. III, we present a self-contained derivation of exact results in the absence of internal reflections, i.e., for $m = 1$, most of them being known from early works by astrophysicists [1,10]. Section IV is devoted to the study of the large-index-mismatch regime ($m \to 0$ or $m \to \infty$). We derive approximate analytic formulas, which provide very accurate results, even for moderate values of the ratio m of optical indices. This analysis also demonstrates the asymptotic validity of the improved diffusion approach. In Sec. V we compare our analytic predictions to numerical results, obtained by a solution of the relevant integral equations. Section VI closes up with a discussion.

II. MICROSCOPIC TREATMENT OF INTERNAL REFLECTIONS

The usual microscopic description of diffusive transport consists in resumming the so-called diffuse ladder diagrams of a systematic multiple-scattering expansion. These diagrams are dominant for the long-distance physics, i.e., length scales much larger than the mean free path, and they lead to the ladder approximation for the Bethe-Salpeter equation [11] for light propagation through a multiply scattering medium in the absence of internal reflections. This procedure provides a microscopic basis for the macroscopic transport equation, introduced by astrophysicists in the 1930s, under the name of radiative transfer theory. For the geometry of a slab limited by two parallel planes, this approach reproduces the well-known one-dimensional Schwarzschild-Milne equation [1].

The main goal of the present work is to extend the above approach to the case where the optical index takes different values inside the diffusive medium and outside. In this situation, the index mismatch generates internal reflections. We are thus led to study the same scattering events, but they have a different weight.

A. Generalities

We study the propagation of scalar waves and consider first a semi-infinite random medium, namely the half-space $z > 0$. It contains a density n of isotropic point scatterers, with scattering length u, situated at uncorrelated random positions. The scattering mean free path is thus equal to $l = 4\pi/(nu^2)$. We make the assumption that the density of scatterers is small, so that l is much larger than the wavelength λ_0 of light inside the medium. The present study only involves the microscopic scattering mechanism through the mean free path l. In particular, because scattering is isotropic, we do not need to distinguish between transport mean free path and scattering mean free path. The general case of anisotropic scattering will be considered briefly in Sec. II G.

The optical index is assumed to take two different values, namely n_0 inside the diffusive medium ($z > 0$) and n_1 outside ($z < 0$). We introduce the ratio $m = n_0/n_1$ of both optical indices.

After averaging over the random positions of the scatterers, the mean-amplitude Green's function inside the medium obeys the equation

$$\left[\frac{\partial^2}{\partial z^2} - \mathbf{q}^2 + \left(k_0 + \frac{i}{2l} \right)^2 \right] G(z, z'; \mathbf{q}) = -\delta(z - z')$$

$$(z > 0), \quad (2.1)$$

where $\mathbf{q}$ is the transversal wave vector, obtained by a Fourier transformation with respect to the transversal coordinates $\rho = (x, y)$. We denote by $k_1 = 2\pi/\lambda_1 = \omega n_1/c$ the wave number of light outside the random medium, c being the velocity of light in vacuum. Similarly, $k_0 = mk_1 = 2\pi/\lambda_0 = \omega n_0/c$ denotes the real part of the wave number inside the medium. In the present framework, the small imaginary part $1/(2l)$ of that wave number is the only manifestation of the presence of a small density of point scatterers. The transversal wave vector $\mathbf{q}$ is conserved across the boundary, leading to the Snell or Descartes law

$$|\mathbf{q}| = q = k_1 \sin \theta = k_0 \sin \theta', \qquad (2.2)$$

where θ is the incidence angle of the incident beam, measured with respect to normal incidence, and θ' is the corresponding angle, measured inside the medium. These definitions are illustrated in Fig. 1, and listed in Table I, together with other useful notations.

We consider the scattering of a plane wave, with unit amplitude, and transversal wave vector $\mathbf{q}_a$, incident from
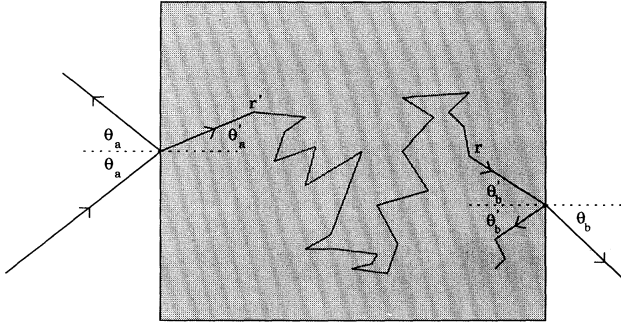
FIG. 1. Schematic plot of multiple scattering in a slab geometry, defining the various incidence angles listed in Table I. A beam incident at an angle θ_a generates a specularly reflected beam and a diffracted beam with incidence angle θ'_a. After diffusive transport has taken place, a wave approaching the interface at an angle θ'_b generates an internally reflected wave and an outgoing beam at an angle θ_b.

the left ($z = -\infty$). Throughout the following, the index a (b) will refer to the incident (outgoing) beam.

Because of the index mismatch, the incident beam generates a reflected and a refracted beam, so that we have the following amplitudes

$$\phi_{\rm in}(\mathbf{r}) = \begin{cases} e^{i\mathbf{q}_a \cdot \rho + i p_a z} - \dfrac{P_a - p_a}{P_a + p_a} e^{i\mathbf{q}_a \cdot \rho - i p_a z} & (z < 0) \\[2ex] \dfrac{2 p_a}{P_a + p_a} e^{i\mathbf{q}_a \cdot \rho + i P_a z} & (z > 0), \end{cases}$$

$$(2.3)$$

with

$$P^2 = \left(k_0 + \frac{i}{2l}\right)^2 - \mathbf{q}^2, \qquad p^2 = k_1^2 - \mathbf{q}^2. \quad (2.4)$$

The intensity of the refracted incident beam decays exponentially inside the medium, according to

$$I_{\rm in}(\mathbf{r}) = |\phi_{\rm in}(\mathbf{r})|^2 = \frac{p_a T_a}{P_a} e^{-z/(l\mu_a)}. \quad (2.5)$$

In this formula, which expresses the Lambert-Beer law, $T_a = T(\mathbf{q}_a)$ is the transmission coefficient, given in Table I. Since we are interested in the regime $k_0 l \gg 1$, we have omitted the small imaginary part of the wave vector P. We shall do so whenever this is possible. This approximation will be shown to be compatible with the conservation of flux, as testified by the sum rules (2.27) and (2.36). Notice, however, that the imaginary part under consideration is needed to obtain the leading exponential decay in Eq. (2.5).

The starting point of the analysis is the following observation. The solution of Eq. (2.1) inside the medium ($z, z' > 0$) simply consists of a "charge" term and a "mirror charge" term, namely

$$G(z, z'; \mathbf{q}) = \frac{i}{2P} \left[e^{iP|z-z'|} + \frac{P-p}{P+p} e^{iP(z+z')} \right]$$

$$(z > 0, \quad z' > 0). \quad (2.6)$$

The prefactor of the second term in Eq. (2.6) is the Fresnel reflection amplitude. In order to evaluate the reflected or transmitted intensity, we shall also need the mean amplitude Green's function for a source at $z > 0$ inside the medium, emitting in a direction defined by $\mathbf{q}$ at an abscissa $z' < 0$. This quantity reads

TABLE I. Definitions and expressions of kinematic and other quantities related to an incident or an outgoing light beam, inside and outside the diffusive medium. Some of the notations are illustrated by Fig. 1.

Quantity	Outside medium	Inside medium
Optical index	n_1	$n_0 = m n_1$
Wave number	$k_1 = n_1 \omega / c$	$k_0 = n_0 \omega / c = m k_1$
Incidence angle	θ	θ'
Parallel wave vector	$p = k_1 \cos\theta$ $= k_0 \sqrt{\mu^2 - 1 + 1/m^2}$	$P = k_0 \cos\theta'$ $= k_0 \mu$
Total-reflection condition	$m < 1$ and $\sin\theta > m$ (i.e., P imaginary)	$m > 1$ and $\sin\theta' > 1/m$ (i.e., p imaginary)
Transverse wave vector	$|\mathbf{q}| = q = k_1 \sin\theta = k_0 \sin\theta' = k_0 \sqrt{1 - \mu^2}$	
Reflection and transmission coefficients	Partial reflection	$\begin{cases} R = \left(\dfrac{P-p}{P+p}\right)^2 = \left(\dfrac{\mu - \sqrt{\mu^2 - 1 + 1/m^2}}{\mu + \sqrt{\mu^2 - 1 + 1/m^2}}\right)^2, \\[2ex] T = \dfrac{4Pp}{(P+p)^2} = \dfrac{4\mu\sqrt{\mu^2 - 1 + 1/m^2}}{(\mu + \sqrt{\mu^2 - 1 + 1/m^2})^2} \end{cases}$
	Total reflection	$\begin{cases} R = 1, \\ T = 0 \end{cases}$

$$G(z, z'; \mathbf{q}) = \frac{i}{P+p} e^{iPz - ipz'} \qquad (z' < 0 < z). \qquad (2.7)$$

B. Transport equation

The diffuse intensity $\Phi(\mathbf{r})$ is the key quantity of the problem. Indeed, predictions concerning physical quantities (reflection, transmission, enhanced backscattering) will follow from the study of $\Phi(\mathbf{r})$, which obeys a transport equation, to be derived below.

As mentioned in the beginning of this section, we restrict the analysis to the ladder approximation to the Bethe-Salpeter equation, which amounts to resumming the ladder diagrams [11]. Within this framework, we are led to consider the following integral equation:

$$\Phi(\mathbf{r}) = \frac{4\pi}{l} \left[I_{\text{in}}(\mathbf{r}) + \int |G(\mathbf{r}, \mathbf{r}')|^2 \Phi(\mathbf{r}') d^3 \mathbf{r}' \right]. \qquad (2.8)$$

The first term on the right-hand side (rhs) of Eq. (2.8) is a source term, which describes first-order scattering of the incoming intensity. All the higher-order scattering events—in the ladder approximation—are generated by iterating this equation.

We consider from now on the situation where the diffusive medium is either a slab of thickness L or a half-space (for $L = \infty$). The diffuse intensity $\Phi(\mathbf{r})$ then only depends on z or rather, as a matter of fact, on the ratio z/l. We thus define the optical depth $\tau = z/l$ and the optical thickness $b = L/l$, and we set

$$\Phi(\mathbf{r}) = \frac{4\pi}{l} \frac{p_a T_a}{P_a} \Gamma(\tau). \qquad (2.9)$$

Let us now insert the form (2.6) of the Green's function into Eq. (2.8). We can neglect the crossed terms, since they are found to be rapidly oscillating, and thus subleading for $k_0 l \gg 1$. Moreover, we are led to make this approximation, as well as that described below Eq. (2.5), by considering the Ward identity which relates the kernel $M(\tau, \tau')$ to be defined in Eq. (2.11) to the form of the left-hand side of Eq. (2.1) [11].

The remaining diagonal terms yield the following integral equation, which generalizes the known Schwarzschild-Milne equation [1,10]

$$\Gamma(\tau) = e^{-\tau/\mu_a} + \int_0^b M(\tau, \tau') \Gamma(\tau') d\tau', \qquad (2.10)$$

where the source term $\exp(-\tau/\mu_a)$ describes the decay of the incident beam, according to Eq. (2.5). $\Gamma(\tau)$ thus represents the normalized diffuse intensity, scattered at a distance $z = l\tau$, induced by a normalized plane wave, incident under an angle θ_a.

In the following, Eq. (2.10) will be referred to as the Milne equation of the problem. The Milne kernel $M(\tau, \tau')$ has a bulk contribution M_B, coming from the charge term in the expression (2.6) of the Green's function, which is already present in the absence of internal reflections, and two layer contributions M_L, which orig-

inate in the mirror charge terms. For isotropic point scattering, we have

$$M(\tau, \tau') = M_B(\tau, \tau') + M_L(\tau, \tau') + M_L(b - \tau, b - \tau'), \qquad (2.11)$$

with

$$M_B(\tau, \tau') = \int_0^1 \frac{d\mu}{2\mu} e^{-|\tau - \tau'|/\mu},$$

$$M_L(\tau, \tau') = \int_0^1 \frac{d\mu}{2\mu} R(\mu) e^{-(\tau + \tau')/\mu}. \qquad (2.12)$$

The Milne kernels can be interpreted as follows. The bulk kernel M_B originates in the angular average of the Lambert-Beer law (2.5), for intensity generated at an optical depth τ' and arriving at a depth τ without having been scattered. The layer kernel M_L describes intensity which has been reflected once at the interface, whence the occurrence of the intensity reflection coefficient $R(\mu)$, given in Table I. The layer kernel decays exponentially away from the boundary; it therefore represents a surface effect, which is only important in the skin layers ($z \sim l$, and $L - z \sim l$ in the case of a slab with finite thickness $L = bl$). However, even when the system is optically thick ($L \gg l$, i.e., $b \gg 1$), internal reflections lead, via the layer kernel M_L, to effects of order unity. We shall now explain how physical quantities can be related to solutions of Eq. (2.10).

C. Diffuse reflection

We consider first the reflected intensity, in the case of a half-space geometry ($b \to \infty$). The Milne equation (2.10) has a special solution $\Gamma_S(\mu_a; \tau)$, whereas the associated homogeneous equation (with no source term) has a solution $\Gamma_H(\tau)$, with the following asymptotic behavior for large depths:

$$\begin{aligned} \Gamma_H(\tau) &\approx \tau + \tau_0, \\ \Gamma_S(\mu_a; \tau) &\approx \tau_1(\mu_a) \end{aligned} \qquad (2.13)$$

($\tau \to \infty$). The additive constant τ_0 depends only on the ratio m of indices in the present case of isotropic scattering. $\tau_1(\mu_a)$ also depends on the direction of the incident beam. Both parameters will be given an interpretation below.

It is advantageous to relate the functions defined above to the special Green's function $G_S(\tau, \tau')$ of the Milne equation. This quantity is defined as the solution of the following equation:

$$G_S(\tau, \tau') = \delta(\tau - \tau') + \int_0^\infty M(\tau, \tau'') G_S(\tau'', \tau') d\tau'', \qquad (2.14)$$

with the condition that $G_S(\tau, \tau')$ remains finite as τ or τ' goes to infinity. It has the symmetry property

$$G_S(\tau, \tau') = G_S(\tau', \tau), \qquad (2.15)$$

as well as the following limit:

$$\lim_{\tau' \to \infty} G_S(\tau, \tau') = \frac{1}{D}\Gamma_H(\tau). \qquad (2.16)$$

The prefactor of this last result has been determined using the diffusion approximation, which yields the simple behavior $G_S(\tau, \tau') = (1/D)\min(\tau, \tau')$ in the long-distance regime $(\tau, \tau', |\tau - \tau'| \gg 1)$. The diffusion coefficient D reads, in reduced units,

$$D = \frac{1}{2} \int_{-\infty}^{\infty} M_B(\tau, 0)\tau^2 d\tau = \frac{1}{3}, \qquad (2.17)$$

i.e., $D = cl/3$ in physical units. Within the present work, i.e., to leading order in the density n of scatterers, the reduction of the speed of light due to scattering resonances [3] is negligible.

As a consequence of the above definitions, we have

$$\Gamma_S(\mu; \tau) = \int_0^{\infty} G_S(\tau, \tau')e^{-\tau'/\mu} d\tau', \qquad (2.18)$$

and in particular, using Eq. (2.16),

$$\tau_1(\mu) = \frac{1}{D} \int_0^{\infty} \Gamma_H(\tau)e^{-\tau/\mu} d\tau. \qquad (2.19)$$

The diffuse reflected intensity for a half-space geometry can be evaluated as follows. We assume for a while that the cross section of the sample is a finite rectangle, with area $\mathcal{A}$, and that periodic transverse boundary conditions are employed. This leads to a quantization of the wave vector $\mathbf{q}$, which assumes discrete values. The reflected intensity at a point $\mathbf{r}' = (z', \boldsymbol{\rho}')$, with $z' < 0$, reads

$$I_R(z', \boldsymbol{\rho}') = \int_0^{\infty} dz \int d^2\rho \, \Phi(z, \boldsymbol{\rho})|G(z, \boldsymbol{\rho}; z', \boldsymbol{\rho}')|^2$$

$$= \int_0^{\infty} dz \int d^2\rho \, \Phi(z, \boldsymbol{\rho})\frac{1}{\mathcal{A}^2}$$

$$\times \sum_{\mathbf{q}, \mathbf{q}'} G(z, z'; \mathbf{q})G^*(z, z'; \mathbf{q}')$$

$$\times e^{i(\mathbf{q} - \mathbf{q}')(\boldsymbol{\rho} - \boldsymbol{\rho}')}. \qquad (2.20)$$

The integration over $\boldsymbol{\rho}$ leads to the condition $\mathbf{q} = \mathbf{q}' = \mathbf{q}_b$, and thus, using Eq. (2.7),

$$I_R(z', \boldsymbol{\rho}') = \frac{1}{\mathcal{A}} \sum_{\mathbf{q}_b} \frac{1}{(P_b + p_b)^2} \int_0^{\infty} \Phi(z)e^{-k_0 z/(P_b l)} dz. \qquad (2.21)$$

As expected, this result is independent of the point $(z', \boldsymbol{\rho}')$. Using $|\mathbf{q}_b| = k_1 \sin\theta_b$ and the substitution

$$\frac{1}{\mathcal{A}} \sum_{\mathbf{q}_b} \to \int \frac{d^2\mathbf{q}_b}{(2\pi)^2} = \int \frac{k_1^2}{(2\pi)^2} \cos\theta_b d\Omega_b, \qquad (2.22)$$

we obtain the following prediction for the diffuse reflected intensity per solid angle element $d\Omega_b$:

$$\frac{dR(a \to b)}{d\Omega_b} = A^R(\theta_a, \theta_b), \qquad (2.23)$$

with

$$A^R(\theta_a, \theta_b) = \frac{\cos\theta_a}{4\pi m^2} \frac{T_a T_b}{\mu_a \mu_b} \gamma(\mu_a, \mu_b) \qquad (2.24)$$

and

$$\gamma(\mu_a, \mu_b) = \int_0^{\infty} \Gamma_S(\mu_a; \tau)e^{-\tau/\mu_b} d\tau$$

$$= \int_0^{\infty} \int_0^{\infty} G_S(\tau, \tau')e^{-\tau/\mu_a} d\tau \, e^{-\tau'/\mu_b} d\tau'. \qquad (2.25)$$

The function $\gamma(\mu_a, \mu_b)$ is defined by Eq. (2.25) for any positive values of its arguments μ_a and μ_b, although these variables have the physical meaning given in Table I, i.e., $\mu = \cos\theta'$, only when they are smaller than unity. It is worth noticing the following relationship between $\gamma(\mu_a, \mu_b)$ and $\tau_1(\mu)$:

$$\tau_1(\mu_a) = \lim_{\mu_b \to \infty} \frac{\gamma(\mu_a, \mu_b)}{\mu_b}, \qquad (2.26)$$

which is a consequence of Eqs. (2.16), (2.19), and (2.25).

The result (2.24) obeys the following sum rule:

$$\int A^R(\theta_a, \theta_b) \cos\theta_b d\Omega_b = T_a \cos\theta_a, \qquad (2.27)$$

which expresses the conservation of flux in the z direction, since the flux of the incident beam (of the beam generated by specular reflection) reads $\cos\theta_a$ $(R_a \cos\theta_a)$.

The sum rule (2.27) assumes a simpler form in terms of the coefficient $\gamma(\mu_a, \mu_b)$ defined in Eq. (2.25), namely

$$\mu_a = \int_0^1 \frac{d\mu_b}{2} T(\mu_b)\gamma(\mu_a, \mu_b). \qquad (2.28)$$

This formula can be proven by means of the following identity:

$$\int_0^1 \frac{d\mu_b}{2} T(\mu_b)e^{-\tau'/\mu_b} = 1 - \int_0^{\infty} M(\tau', \tau'') d\tau'', \qquad (2.29)$$

and by using then Eq. (2.14) for the Green's function $G_S(\tau, \tau')$, together with its symmetry property (2.15).

Finally, by comparing Eqs. (2.26) and (2.28), we obtain the following identity:

$$\int_0^1 \frac{d\mu}{2} T(\mu)\tau_1(\mu) = 1. \qquad (2.30)$$

D. Diffuse transmission and electrical conductance

Consider now the geometry of an optically thick slab, of thickness $L = bl$, with $b \gg 1$. The solution of Eq. (2.10) for such a geometry can be constructed from the solutions in a half-space by means of a matching pro-

cedure commonly used for diffusion equations. In the present case, the matching conditions are determined by the asymptotic form (2.13) of the solutions of Eq. (2.10) for $b = \infty$. We thus obtain the solution pertaining to a thick slab

$$\Gamma(\tau) \approx \begin{cases} \Gamma_S(\mu_a; \tau) - \dfrac{\tau_1(\mu_a)}{b + 2\tau_0}\Gamma_H(\tau) & (0 \leq \tau \leq b/2) \\[3mm] \dfrac{\tau_1(\mu_a)}{b + 2\tau_0}\Gamma_H(b - \tau) & (b/2 \leq \tau \leq b). \end{cases}$$
$$(2.31)$$

Both expressions of Eq. (2.31) lead to the linear (diffusive) behavior

$$\Gamma(\tau) = \frac{\tau_1(\mu_a)}{b + 2\tau_0}(b + \tau_0 - \tau) + O\left(e^{-\tau}, e^{-(b-\tau)}\right) \quad (2.32)$$

in the bulk of the sample, whereas the precise form of the solutions Γ_H and Γ_S describes the intensity profile in the skin layers, i.e., in the vicinity of both boundaries ($\tau \sim 1$ and $b - \tau \sim 1$). The result (2.31) also exhibits explicitly the conservation of flux. Indeed, for a finite optical thickness b, the transmitted flux is simply subtracted from the reflected one.

The result (2.32) suggests to interpret τ_0 as the effective dimensionless thickness of one skin layer. Indeed, the denominator $b + 2\tau_0$ is a measure of the apparent optical thickness of the slab. This physical interpretation will become more evident when considering, e.g., the example of the electrical conductance, at the end of this section.

The diffuse transmitted intensity can be evaluated in analogy with the diffuse reflected intensity, namely by considering first the case of a large but finite sample cross section $\mathcal{A}$. We thus obtain, along the lines of Eqs. (2.20)–(2.22), and using also Eq. (2.19),

$$\frac{dT(a \to b)}{d\Omega_b} = \frac{A^T(\theta_a, \theta_b)}{b + 2\tau_0}, \quad (2.33)$$

with

$$A^T(\theta_a, \theta_b) = \frac{\cos\theta_a}{12\pi m^2}\frac{T_a T_b}{\mu_a \mu_b}\tau_1(\mu_a)\tau_1(\mu_b). \quad (2.34)$$

The expression (2.34) of the diffuse transmission also fulfills a sum rule, which is similar to some extent to Eq. (2.27). Indeed, define the total flux transmission T_{flux} as follows:

$$T_{\text{flux}} = \sum_{\mathbf{q}_a, \mathbf{q}_b} T_{\mathbf{q}_a, \mathbf{q}_b}\frac{\cos\theta_b}{\cos\theta_a}. \quad (2.35)$$

Using again the procedure of Eqs. (2.20)–(2.22), together with the identity (2.30), we obtain the following result:

$$T_{\text{flux}} = \frac{k_0^2}{3\pi}\frac{\mathcal{A}}{b + 2\tau_0}. \quad (2.36)$$

This formula provides an exact sum rule for the diffuse intensity, which has an interesting physical interpretation.

Consider indeed a metallic sample with a slab geometry, at zero temperature, with a small concentration of elastic scatterers. The present formalism applies to such a situation, in the regime where the phase coherence length is very large ($L \ll L_\phi$), up to the replacement of k_0 by the Fermi wave vector k_F. In this problem, the analog of a mismatch between optical indices is a difference between the potentials in the sample ($V = V_0$) and in the leads ($V = V_1$). The parameter m^2 should now be interpreted as $(k_F^2 - V_0)/(k_F^2 - V_1)$. The conductance G of the sample can be evaluated by means of the multichannel Landauer formula [12], namely

$$G = \frac{2e^2}{h}T_{\text{flux}} = \frac{\mathcal{A}}{L + 2\tau_0 l}\sigma_B, \quad (2.37)$$

where

$$\sigma_B = \frac{2e^2 k_F^2 l}{3\pi h} \quad (2.38)$$

is known as the Boltzmann conductivity, in spite of its quantum character [13].

It is more suggestive to express the resistance $R = 1/G$ of the sample as

$$R = \frac{L}{\sigma_B \mathcal{A}} + 2R_C. \quad (2.39)$$

The first term of this expression is the bulk contribution, which has the usual length-over-area form, referred to as Ohm's law, whereas the second contribution shows that the skin layers generate two extra boundary resistances, or contact resistances, R_C, namely

$$R_C = \frac{3\pi h}{2e^2 \mathcal{A} k_F^2}\tau_0. \quad (2.40)$$

The above expression shows that R_C is proportional to the dimensionless thickness τ_0 of the skin layer and inversely proportional to the number $N \approx \mathcal{A}k_F^2/(2\pi)^2$ of open channels across the sample.

E. Enhanced backscattering cone

The above formalism can be extended to the prediction of various correlation functions pertaining to the multiple-scattering problem. Let us focus our attention onto the enhanced backscattering which takes place in the vicinity of the exact backward direction ($\mathbf{q}_b = \mathbf{q}_a$), in an angular domain of order $\theta \sim 1/(k_0 l) \ll 1$. This yields the celebrated enhanced backscattering cone [14,15].

Restricting the analysis to normal incidence ($\mathbf{q}_a = \mathbf{0}$) and to a half-space diffusive medium, for the sake of simplicity, we set $q_b = Q/l$, where

$$Q = k_0 l\theta_b' = k_1 l\theta_b \quad (2.41)$$

is the dimensionless scattering wave vector.

For a normalized incident plane wave, the diffusive intensity in the vicinity of the exact backscattering direction consists in [7,16] (i) a background term, given by

the result (2.24) for the diffuse reflected intensity, namely $A^R(0,0) = T(1)^2\gamma(1,1)/(4\pi m^2)$; and (ii) an extra contribution, called enhanced backscattering and given by

$$A^C(Q) = \frac{T(1)^2}{4\pi m^2}\left[\gamma_C(Q) - \frac{1}{2}\right]. \qquad (2.42)$$

It turns out that the maximal value $\gamma_C(0)$ coincides with the background contribution $\gamma(1,1)$. The physical explanation of this property is as follows. In the backscattering direction, every path is in phase with its time-reversed counterpart, whence a doubling of the amplitude. This argument does not hold for a subclass of scattering events, which are their own time-reversed transforms. In the low-density limit, only the single-scattering events have to be discarded. The reflected intensity at exact backscattering is therefore enhanced by a factor that is slightly below 2, because of the subtraction made in Eq. (2.42) of the term $1/2$, representing the contribution of the single-scattering events.

Let us make the content of the result (2.42) more explicit. We have [7,16,17]

$$\gamma_C(Q) = \int_0^\infty \Gamma_C(Q;\tau)e^{-\tau}\,d\tau, \qquad (2.43)$$

where $\Gamma_C(Q;\tau)$ is the solution of the Q-dependent Milne equation

$$\Gamma_C(Q;\tau) = e^{-\tau} + \int_0^\infty M(Q;\tau,\tau')\Gamma_C(Q;\tau')\,d\tau'. \qquad (2.44)$$

The Milne kernel still consists of two parts, just as in Eq. (2.11), namely

$$M_B(Q;\tau,\tau') = \int_0^1 \frac{d\mu}{2\mu}J_0\left(Q|\tau-\tau'|\sqrt{1-\mu^2}/\mu\right)$$
$$\times\, e^{-|\tau-\tau'|/\mu},$$
$$M_L(Q;\tau,\tau') = \int_0^1 \frac{d\mu}{2\mu}J_0\left[Q(\tau+\tau')\sqrt{1-\mu^2}/\mu\right]$$
$$\times\, R(\mu)e^{-(\tau+\tau')/\mu}, \qquad (2.45)$$

where $J_0(z)$ is the Bessel function of zeroth order.

The behavior of the amplitude $\gamma_C(Q)$ at normal incidence in the limit of small and large values of the reduced wave vector Q can be obtained as follows. For Q large, both kernels exhibit a fast decay: $M_B(Q;\tau,0) \sim M_L(Q;\tau,0) \sim \exp(-|Q\tau|)$. As a consequence, the backscattering amplitude can be approximated by the first orders of the multiple-scattering expansion, namely [18,19]

$$\gamma_C(Q) = \frac{1}{2} + \int_0^\infty\int_0^\infty M(Q;\tau,\tau')e^{-\tau}\,d\tau\;e^{-\tau'}\,d\tau' + \cdots$$
$$= \frac{1}{2} + \frac{\pi}{4Q} + \left[\frac{1}{2}\frac{(m-1)^2}{(m+1)^2} - 1\right]\frac{1}{Q^2} + \cdots$$

$$(|Q| \to \infty). \quad (2.46)$$

This result implies that $A^C(Q)$ falls off as $1/|Q|$ for large

Q. The backscattering cone is thus a narrow peak on top of a smooth background.

The opposite regime of a small reduced wave vector Q can be dealt with as follows. We notice first that $\Gamma_C(Q;\tau)$ coincides with $\Gamma_S(1;\tau)$ for $Q=0$, so that $\gamma_C(0) = \gamma(1,1)$, as announced above. For small values of Q, the backscattering amplitude exhibits the celebrated triangular shape

$$\gamma_C(Q) = \gamma(1,1)\left(1 - \frac{|Q|}{\Delta Q} + \cdots\right) \qquad (Q \to 0), \quad (2.47)$$

which is a consequence of the following linear behavior:

$$\Gamma_C(Q;\tau) = \Gamma_S(1;\tau) - \tau_1(1)\Gamma_H(\tau)|Q| + \cdots \qquad (Q \to 0). \quad (2.48)$$

The prefactor of the term involving $\Gamma_H(\tau)$ has been fixed by matching the expansion (2.48) with the expected behavior $\Gamma_C(Q;\tau) \approx C(Q)\exp(-|Q|\tau)$ at large τ, where the amplitude $C(Q)$ has a finite limit for $Q \to 0$, which has to coincide with $\tau_1(1)$. We thus obtain the following expression:

$$\Delta Q = \frac{3\gamma(1,1)}{[\tau_1(1)]^2} \qquad (2.49)$$

for the reciprocal slope of the cone at its top [17].

The full shape of the backscattering cone can be obtained by solving the Milne equation (2.44). This will be done in the following, either exactly in the absence of internal reflections [20] (see Sec. III) and approximately or numerically in the general case (see Secs. IV and V).

F. The air-glass-medium interface

The above approach can be generalized to other experimental situations involving internal reflections, such as that of a fluid diffusive medium, which is necessarily enclosed in a transparent cell, usually made of glass. Internal reflections can then occur both at the fluid-glass interface and at the glass-air interface. The latter reinject partly the outgoing intensity into the medium.

The effects of both types of internal reflections can be easily taken into account in the framework of the present analysis. We consider for definiteness a planar double interface (air-glass-medium) with thickness d. We denote by n_i the optical index of the medium number i, where $i = 0$ corresponds to the random scattering medium ($z > 0$); $i = 1$ corresponds to the outer medium (air) ($z < -d$); and $i = 2$ corresponds to the intermediate layer (glass) ($-d < z < 0$).

Consider a normalized beam, incident from the air. It is characterized by a transversal wave vector $\mathbf{q}$ and three longitudinal wave vectors p_i, with $p_i^2 + \mathbf{q}^2 = k_i^2$, and $k_i = \omega n_i/c$. The amplitudes of this beam in the three media assume the form

$$\phi_{\rm in}(\mathbf{r}) = \begin{cases} e^{i\mathbf{q}\cdot\rho+ip_1 z} + re^{i\mathbf{q}\cdot\rho-ip_1 z} & (z < -d) \\ t_1 e^{i\mathbf{q}\cdot\rho+ip_2 z} + t_2 e^{i\mathbf{q}\cdot\rho-ip_2 z} & (-d < z < 0) \\ t e^{i\mathbf{q}\cdot\rho+ip_0 z} & (z > 0). \end{cases}$$

$$(2.50)$$

In this formula,

$$r = \frac{(p_0 + p_2)(p_1 - p_2) - (p_0 - p_2)(p_1 + p_2)e^{2ip_2d}}{(p_0 + p_2)(p_1 + p_2) - (p_0 - p_2)(p_1 - p_2)e^{2ip_2d}}$$
$$\times e^{-2ip_1d},$$

$$t = \frac{4p_1p_2e^{i(p_2 - p_1)d}}{(p_0 + p_2)(p_1 + p_2) - (p_0 - p_2)(p_1 - p_2)e^{2ip_2d}}$$

$$(2.51)$$

are the amplitude reflection and transmission coefficients. The expressions for t_1 and t_2, which describe the beams inside the glass pane, will not be needed.

In practical situations, the thickness d of the glass layer is not fixed within optical precision. Hence we are led to define a mean intensity reflection coefficient R_3 and a mean intensity transmission coefficient T_3 through

$$R_3 = \langle |r|^2 \rangle, \qquad T_3 = \frac{p_0}{p_1} \langle |t|^2 \rangle, \qquad (2.52)$$

where the brackets represent a uniform averaging over the phase $2p_2d$. We thus get

$$T_3 = 1 - R_3 = \frac{4p_0p_1p_2}{(p_0 + p_1)(p_0p_1 + p_2^2)}. \qquad (2.53)$$

It is worth noticing that the results of Table I for $R(\mu)$ and $T(\mu)$ are recovered in the case $p_1 = p_2 = p$, $p_0 = P = k_0\mu$.

The predictions exposed above concerning the influence of skin layers can be extended to the present case by making use of the expressions (2.53) at suitable places, namely by replacing the transmission coefficients T_a and T_b by the expression (2.53) for T_3, with values of the p_i determined by the directions of the incident and outgoing beams; and the reflection coefficient $R(\mu)$ in Eqs. (2.12) and (2.45) for the layer Milne kernels by the expression (2.53) for R_3, with $\mu = p_0/k_0$.

G. Anisotropic scattering and the radiative transfer equation

Until now we have studied only the case of isotropic scattering. In more realistic situations, an anisotropic scattering cross section has to be considered. In the very dilute regime considered in this work, the scatterers can still be assumed to be pointlike. Their scattering cross section has an angular dependence, which can be decomposed in the usual form

$$\sigma(\mu, \varphi; \mu', \varphi') = u^2 p(\mu, \varphi; \mu', \varphi'), \qquad (2.54)$$

where $\mu = \cos\theta$ and φ (μ' and φ') denote the direction of the outgoing (incoming) wave in the laboratory coordinate frame. The notations used throughout this section have been chosen because they are standard ones, rather than for their accord with other sections.

The angular factor p is normalized so that

$$\int_{-1}^{1} \frac{d\mu}{2} \int_0^{2\pi} \frac{d\varphi}{2\pi} p(\mu, \varphi; \mu', \varphi') = 1. \qquad (2.55)$$

It turns out that p depends only on the relative scattering angle, both for isotropic scattering and for anisotropic scattering after averaging over all orientations of the scatterers. Then the φ and φ' dependence of p can be integrated out. We thus define

$$p_0(\mu; \mu') = \int_0^{2\pi} \frac{d\varphi}{2\pi} \int_0^{2\pi} \frac{d\varphi'}{2\pi} p(\mu, \varphi; \mu', \varphi'). \qquad (2.56)$$

The transport equation is usually presented in the literature [1,2,10] under a form which is local in τ, and known as the radiative transfer equation. Let $I(\tau, \mu')$ denote the normalized specific intensity arriving at an optical depth τ in direction μ', φ', averaged over φ'. The radiative transfer equation reads

$$\mu' \frac{\partial}{\partial \tau} I(\tau, \mu') + I(\tau, \mu') = \int_{-1}^{1} \frac{d\mu''}{2} p_0(\mu'; \mu'') I(\tau, \mu'').$$

$$(2.57)$$

Because of the presence of internal reflections at the interfaces, Eq. (2.57) has to be complemented by the following boundary conditions at $\tau = 0^+$ and $\tau = b^-$:

$$I(0^+, \mu') = \delta(\mu' - \mu_a)$$
$$+ R(\mu') \int_0^b d\tau' e^{-\tau'/\mu'}$$
$$\times \int_{-1}^{1} \frac{d\mu''}{2} p_0(-\mu'; \mu'') I(\tau', \mu''),$$

$$(2.58)$$

$$I(b^-, -\mu') = R(-\mu') \int_0^b d\tau' e^{-(b-\tau')/\mu'}$$
$$\times \int_{-1}^{1} \frac{d\mu''}{2} p_0(\mu'; \mu'') I(\tau', \mu''),$$

where μ_a characterizes the direction of the incident beam and $R(\mu')$ is the intensity reflection coefficient given in Table I.

We now introduce the intensity $\Gamma(\tau, \mu)$ scattered at the depth τ into the direction μ, namely

$$\Gamma(\tau, \mu) = \int_{-1}^{1} \frac{d\mu'}{2} p_0(\mu; \mu') I(\tau, \mu'). \qquad (2.59)$$

In the case of isotropic scattering, i.e., $p_0(\mu, \mu') = 1$ for all μ and μ', the quantity defined in Eq. (2.59) reduces to the diffuse intensity $\Gamma(\tau)$ introduced in Eq. (2.9). In the present situation, $\Gamma(\tau, \mu)$ also depends implicitly on the direction μ_a of the incident beam. It should, of course, not be confused with the function $\Gamma_S(\mu_a; \tau)$ introduced in Eq. (2.13).

The quantity $\Gamma(\tau, \mu)$ satisfies the following generalized Schwarzschild-Milne integral equation:

$$\Gamma(\tau,\mu) = p_0(\mu;\mu_a)e^{-\tau/\mu_a} + \int_0^\tau d\tau' \int_0^1 \frac{d\mu'}{2\mu'} p_0(\mu;\mu')e^{-|\tau-\tau'|/\mu'}\Gamma(\tau',\mu')$$

$$+ \int_\tau^b d\tau' \int_0^1 \frac{d\mu'}{2\mu'} p_0(\mu;-\mu')e^{-|\tau-\tau'|/\mu'}\Gamma(\tau',-\mu')$$

$$+ \int_0^b d\tau' \int_0^1 \frac{d\mu'}{2\mu'} R(\mu')p_0(\mu;\mu')e^{-(\tau+\tau')/\mu'}\Gamma(\tau',-\mu')$$

$$+ \int_0^b d\tau' \int_0^1 \frac{d\mu'}{2\mu'} R(-\mu')p_0(\mu;-\mu')e^{-(2b-\tau-\tau')/\mu'}\Gamma(\tau',\mu'). \tag{2.60}$$

The source term and the first two integrals on the rhs of Eq. (2.60) are standard. They represent, respectively, the intensity which is scattered for the first time, the scattered intensity arriving from lower depths ($0 \le \tau' < \tau$), and the scattered intensity arising from higher depths ($\tau < \tau' \le b$). The last two integrals are novel. They are due to the mismatch between optical indices, and more precisely they describe the intensity emitted at an arbitrary depth in the direction of the interface, reflected by the interface, and scattered once, namely at the final depth τ.

A final comment is in order. In solving Eq. (2.57), e.g., numerically, in the general case of anisotropic scattering, the boundary conditions (2.58), which arise from internal reflections at the interface, will have to be taken into account in a self-consistent fashion. Because of the exponential weights $\exp(-\tau'/\mu')$ and $\exp\left[-(2b-\tau-\tau')/\mu'\right]$, this procedure only involves a self-consistent solution in a skin layer, with a thickness of a few mean free paths.

III. EXACT RESULTS IN THE ABSENCE OF INTERNAL REFLECTIONS

This section is devoted to an elementary and self-contained presentation of analytic results concerning the problem of multiple isotropic scattering of scalar waves by point scatterers, in the case where there are no internal reflections ($n_0 = n_1$). This is indeed the only situation where explicit results can be obtained, and have been obtained, to the best of our knowledge. Most of the results exposed in Secs. III A and III B were already known to the astrophysicists' community [1], owing especially to the work of Ambartsumian and Chandrasekhar, whereas some of the results of Secs. III C and III D can be found in Ref. [20]. We have nevertheless found it worthwhile to recover all those results in the present context and to produce elementary derivations for them. We have not found such a compact exposition in the literature.

A. The homogeneous Milne equation

The starting point of this analysis is the integral Schwarzschild-Milne equation (2.10) rather than the radiative transfer formalism exposed in Sec. II G. In the absence of internal reflections, Eq. (2.10) only contains the contribution of the bulk kernel $M_B(\tau,\tau')$, defined in

Eq. (2.12). Since this kernel only depends on the difference $(\tau - \tau')$, the Milne equation has the structure of a convolution equation. The problem is still nontrivial, because of its half-space geometry. This observation suggests nevertheless to utilize the Laplace transformation.

We consider first the homogeneous Milne equation, and we recall that we are interested in its solution $\Gamma_H(\tau)$, which possesses the asymptotic behavior given by Eq. (2.13).

We define the Laplace transforms of $M_B(\tau,0)$ and $\Gamma_H(\tau)$ as follows:

$$m(s) = \int_{-\infty}^\infty M_B(\tau,0)\, e^{s\tau} d\tau \qquad (-1 < \mathrm{Re}\, s < 1), \tag{3.1}$$

$$g_H(s) = \int_0^\infty \Gamma_H(\tau)\, e^{s\tau} d\tau = D\,\tau_1(\mu = -1/s) \ (\mathrm{Re}\, s < 0). \tag{3.2}$$

In the case of isotropic scattering by pointlike objects, the expression (2.12) of the Milne kernel leads to

$$m(s) = \frac{1}{2s} \ln \frac{1+s}{1-s}. \tag{3.3}$$

It turns out that the problem can be solved for any symmetric Milne kernel. The value $m(0)$ is equal to the total albedo, which will be assumed to be unity, except in Sec. III D. The small-s behavior of $m(s)$

$$m(s) = 1 + Ds^2 + O(s^4) \qquad (s \to 0) \tag{3.4}$$

determines the dimensionless diffusion constant D, which reads $D = 1/3$ for isotropic scattering, in accord with Eq. (2.17).

The homogeneous Milne integral equation is equivalent to

$$\phi(s)g_H(s) = \int \frac{dt}{2\pi i} \frac{m(t)g_H(t)}{t-s} \quad (-1 < \mathrm{Re}\, t < \mathrm{Re}\, s < 0), \tag{3.5}$$

with

$$\phi(s) = 1 - m(s), \tag{3.6}$$

and the asymptotic behavior (2.13) is equivalent to

$$s^2 g_H(s) = 1 - \tau_0 s + O(s^2) \qquad (s \to 0). \qquad (3.7)$$

Equation (3.5) can be solved in closed form, for an arbitrary bulk kernel. Let us consider first the following "rational case," where $M_B(\tau, 0)$ is a finite superposition of N decaying exponentials, namely

$$M_B(\tau, 0) = \sum_{a=1}^{N} \frac{w_a p_a}{2} e^{-p_a |\tau|}, \qquad (3.8)$$

with weights $w_a > 0$ and decay rates (inverse correlation lengths) $p_a > 0$. We have then

$$m(s) = \sum_{a=1}^{N} \frac{w_a p_a^2}{p_a^2 - s^2}, \qquad \phi(s) = -s^2 \sum_{a=1}^{N} \frac{w_a}{p_a^2 - s^2}. \qquad (3.9)$$

By comparing with Eq. (3.4), we obtain the normalization conditions

$$\sum_{a=1}^{N} w_a = 1, \qquad \sum_{a=1}^{N} \frac{w_a}{p_a^2} = D. \qquad (3.10)$$

Equation (3.5) can be evaluated by means of residue calculus. It loses its integral nature and becomes

$$\phi(s) g_H(s) = -\sum_{a=1}^{N} \frac{w_a p_a g_H(-p_a)}{2(p_a + s)}. \qquad (3.11)$$

In order to solve Eq. (3.11), we first write the rational function $\phi(s)$ in factorized form, namely

$$\phi(s) = -s^2 \frac{\prod_{\alpha=1}^{N-1} (z_\alpha^2 - s^2)}{\prod_{a=1}^{N} (p_a^2 - s^2)} = \frac{\prod_{\alpha=1}^{N-1} (1 - z_\alpha^2/s^2)}{\prod_{a=1}^{N} (1 - p_a^2/s^2)}. \qquad (3.12)$$

The $(N-1)$ zeros of $[\phi(s)/s^2]$ in the variable s^2 have been denoted by z_α^2, with $\mathrm{Re}\, z_\alpha > 0$, for $1 \le \alpha \le N-1$. The normalization of Eq. (3.12) has been fixed by using $\phi(\infty) = 1$.

An alternative expression for the diffusion constant D can be derived by letting s go to zero in Eq. (3.12), and comparing with Eqs. (3.4) and (3.9). We get

$$D = \frac{\prod_{\alpha=1}^{N-1} z_\alpha^2}{\prod_{a=1}^{N} p_a^2}. \qquad (3.13)$$

The solution of Eq. (3.11) is of the form

$$\phi(s) g_H(s) = \frac{\mathcal{N}_0(s)}{\prod_{a=1}^{N} (p_a + s)}, \qquad (3.14)$$

with $\mathcal{N}_0(s)$ a polynomial of degree $(N-1)$, which can be determined as follows. Consider the value $s = -z_\alpha$: we have $\phi(-z_\alpha) = 0$, whereas $g_H(-z_\alpha)$ is finite. Equation (3.14) shows therefore that $s = -z_\alpha$ is a zero of the

polynomial $\mathcal{N}_0(s)$. Since there are exactly $(N - 1)$ such values, the solution (3.14) is determined up to a normalization, which can be fixed by using Eq. (3.7). We thus obtain

$$s^2 g_H(s) = \frac{\prod_{a=1}^{N} (1 - s/p_a)}{\prod_{\alpha=1}^{N-1} (1 - s/z_\alpha)}. \qquad (3.15)$$

This formula can be recast for $\mathrm{Re}\, s < 0$ as

$$s^2 g_H(s) = \exp \left\{ \sum_{a=1}^{N} \ln(1 - s/p_a) - \sum_{\alpha=1}^{N-1} \ln(1 - s/z_\alpha) \right\}. \qquad (3.16)$$

The sum over the poles and zeros of the function $[\phi(s)/s^2]$, with positive real parts, can be rewritten as the following complex integrals:

$$s^2 g_H(s) = \exp \left\{ \int_{-i\infty}^{+i\infty} \frac{dz}{2\pi i} \left[\frac{\phi'(z)}{\phi(z)} - \frac{2}{z} \right] \ln(1 - s/z) \right\}$$
$$= \exp \left\{ -s \int_{-i\infty}^{+i\infty} \frac{dz}{2\pi i z (z - s)} \ln \left[-\frac{\phi(z)}{Dz^2} \right] \right\}. \qquad (3.17)$$

This result clearly provides the solution of the problem for an arbitrary bulk Milne kernel.

The thickness τ_0 of the skin layer can be evaluated by comparing the results (3.15) and (3.17) with the expansion (3.7). We get

$$\tau_0 = \sum_{a=1}^{N} \frac{1}{p_a} - \sum_{\alpha=1}^{N-1} \frac{1}{z_\alpha} = \int_{-i\infty}^{+i\infty} \frac{dz}{2\pi i z^2} \ln \left[-\frac{\phi(z)}{Dz^2} \right]. \qquad (3.18)$$

The value for the case of point scattering is obtained by inserting into Eq. (3.18) the expression of $\phi(z)$ coming from Eq. (3.3). By making the change of variable $z = i \tan \beta$, we get

$$\tau_0 = \frac{1}{\pi} \int_0^{\pi/2} \frac{d\beta}{\sin^2 \beta} \ln \frac{\tan^2 \beta}{3(1 - \beta \cot \beta)} = 0.710\,446\,090. \qquad (3.19)$$

We recover a well-known numerical value [1,10,21].

B. The inhomogeneous Milne equation

We consider now the inhomogeneous Milne equation (2.10) in the absence of internal reflections. We use the notation μ for the variable μ_a related to the incident beam and recall that we are interested in the special solution $\Gamma_S(\mu; \tau)$, which admits a finite limit $\tau_1(\mu)$, as $\tau \to \infty$, according to Eq. (2.13). We still use the Laplace formalism exposed in Sec. III A and the notations intro-

duced there. We obtain

$$\phi(s)g_S(\mu;s) = \frac{\mu}{1-\mu s} + \int \frac{dt}{2\pi i} \frac{m(t)g_S(\mu;t)}{t-s}$$

$$(-1 < \mathrm{Re}\,t < \mathrm{Re}\,s < 0), \quad (3.20)$$

whereas the asymptotic behavior (2.13) can be recast as

$$\lim_{s\to 0}[-sg_S(\mu;s)] = \tau_1(\mu). \quad (3.21)$$

We consider first the rational Milne kernels, introduced in Eq. (3.8). In such a case, the solution of Eq. (3.20) assumes the form

$$\phi(s)g_S(\mu;s) = \frac{\mu}{1-\mu s} + \frac{\mathcal{N}_1(s)}{\prod\limits_{a=1}^{N}(p_a+s)}, \quad (3.22)$$

where $\mathcal{N}_1(s)$ is a polynomial in s with degree $(N-1)$, yet to be determined. Equation (3.22) implies

$$s^2 g_S(\mu;s) = -\frac{\mathcal{N}(s)}{1-\mu s} \frac{\prod\limits_{a=1}^{N}(p_a-s)}{\prod\limits_{\alpha=1}^{N-1}(z_\alpha^2-s^2)}, \quad (3.23)$$

with

$$\mathcal{N}(s) = (1-\mu s)\mathcal{N}_1(s) + \mu \prod\limits_{a=1}^{N}(p_a+s). \quad (3.24)$$

We observe that $\mathcal{N}(s)$ is a polynomial with degree N, which vanishes for $s=0$, in virtue of Eq. (3.21), and for each of the $(N-1)$ zeros $s = -z_\alpha$ of the function $[\phi(s)/s^2]$. Moreover, the value $\mathcal{N}(1/\mu)$ is known from Eq. (3.24). The above properties determine $\mathcal{N}(s)$. We thus get the following result:

$$g_S(\mu;s) = -\frac{\mu^2}{s(1-\mu s)D}$$

$$\times \frac{\prod\limits_{a=1}^{N}\{(1-s/p_a)[1+1/(\mu p_a)]\}}{\prod\limits_{\alpha=1}^{N-1}\{(1-s/z_\alpha)[1+1/(\mu z_\alpha)]\}}, \quad (3.25)$$

and especially

$$\tau_1(\mu) = \frac{\mu^2}{D} \frac{\prod\limits_{a=1}^{N}[1+1/(\mu p_a)]}{\prod\limits_{\alpha=1}^{N-1}[1+1/(\mu z_\alpha)]}. \quad (3.26)$$

The results (3.25) and (3.26) have the same factorized structure as Eq. (3.15). Their generalization to an arbitrary kernel can be written immediately as complex integrals, in analogy with Eqs. (3.17) and (3.18),

$$g_S(\mu;s) = -\frac{\mu^2}{s(1-\mu s)D}$$

$$\times \exp\left\{\int_{-i\infty}^{+i\infty} \frac{dz}{2\pi i}\left[\frac{\phi'(z)}{\phi(z)} - \frac{2}{z}\right]\right.$$

$$\left. \times \ln\{(1-s/z)[1+1/(\mu z)]\}\right\}, \quad (3.27)$$

$$\tau_1(\mu) = \frac{\mu^2}{D} \exp\left\{\int_{-i\infty}^{+i\infty} \frac{dz}{2\pi i}\left[\frac{\phi'(z)}{\phi(z)} - \frac{2}{z}\right]\right.$$

$$\left. \times \ln[1+1/(\mu z)]\right\}$$

$$= \frac{\mu^2}{D} \exp\left\{\int_{-i\infty}^{+i\infty} \frac{dz}{2\pi i z(1+\mu z)}\right.$$

$$\left. \times \ln\left[-\frac{\phi(z)}{Dz^2}\right]\right\}. \quad (3.28)$$

We notice that the result (3.26) could be derived alternatively by means of Eqs. (3.2) and (3.15).

In the regime of grazing incidence, $\tau_1(\mu)$ vanishes linearly, according to

$$\frac{\tau_1(\mu)}{\mu} \to \frac{\Gamma_H(0)}{D} = \frac{1}{\sqrt{D}} \quad (\mu \to 0), \quad (3.29)$$

in virtue of Eq. (2.19).

For point scattering, we obtain the following result by setting $z = i\tan\beta$ in the second formula of Eq. (3.28):

$$\tau_1(\mu) = \mu\sqrt{3}\,\exp\left\{-\frac{\mu}{\pi}\int_0^{\pi/2} d\beta\,\frac{\ln(1-\beta\cot\beta)}{\cos^2\beta + \mu^2\sin^2\beta}\right\}. \quad (3.30)$$

This quantity is maximal at normal incidence ($\mu = 1$), where it assumes the somewhat simpler form

$$\tau_1(1) = \sqrt{3}\,\exp\left\{-\frac{1}{\pi}\int_0^{\pi/2} d\beta\,\ln(1-\beta\cot\beta)\right\}$$

$$= 5.036\,475\,57. \quad (3.31)$$

Finally, it is worth noticing that Eq. (3.25) also implies the following remarkable result:

$$\gamma(\mu_a,\mu_b) = g_S(\mu_a; s = -1/\mu_b) = \frac{\tau_1(\mu_a)\tau_1(\mu_b)}{3(\mu_a+\mu_b)}, \quad (3.32)$$

which is, of course, particular to the situation where there are no internal reflections.

C. Enhanced backscattering cone

Exact results can also be derived concerning the backscattering cone in the absence of internal reflections [20]. Consider, for the sake of simplicity, the enhanced

backscattering of a normally incident beam ($\mu_a = 1$). The Q-dependent Milne equation (2.44) can be solved by means of the Laplace transformation. We denote by $m(Q; s)$ and $g_C(Q; s)$, respectively, the Laplace transforms of $M_B(Q; \tau, 0)$ and of $\Gamma_C(Q; \tau)$, defined in analogy with Eqs. (3.1) and (3.2).

We start by transforming the integral representation (2.45) of the Milne kernel into the following one, which only involves elementary functions:

$$M_B(Q; \tau, 0) = \frac{1}{2} \int_{x_0}^{\infty} \frac{e^{-x} \, dx}{\sqrt{x^2 - Q^2 \tau^2}}, \qquad (3.33)$$

with $x_0 = \tau\sqrt{1 + Q^2}$. We can derive from Eq. (3.33) the following expressions, which hold for $|\mathrm{Re}\,s| < \sqrt{1 + Q^2}$:

$$\begin{aligned} m(Q; s) &= \frac{\arctan\sqrt{Q^2 - s^2}}{\sqrt{Q^2 - s^2}} \\ &= \frac{1}{2\sqrt{s^2 - Q^2}} \ln\frac{1 + \sqrt{s^2 - Q^2}}{1 - \sqrt{s^2 - Q^2}}. \end{aligned} \qquad (3.34)$$

The Laplace-transformed Q-dependent Milne equation can be solved along the lines of Sec. III B, up to the following difference. The effective albedo $m(Q; 0) = (\arctan Q)/Q$ is smaller than unity, so that we have $\phi(Q; 0) \neq 0$ for $Q \neq 0$. The rational Q-dependent Milne kernels have therefore now exactly N zeros $\{z_\alpha^2\}$ and N poles $\{p_a^2\}$ in the variable s^2, all of them being differ-

ent from zero. For those rational kernels, we obtain the solution

$$g_C(Q; s) = \frac{1}{1 - s} \frac{\displaystyle\prod_{a=1}^{N} [(p_a + 1)(p_a - s)]}{\displaystyle\prod_{\alpha=1}^{N} [(z_\alpha + 1)(z_\alpha - s)]}, \qquad (3.35)$$

and thus

$$\gamma_C(Q) = \frac{1}{2} \frac{\displaystyle\prod_{a=1}^{N} (p_a + 1)^2}{\displaystyle\prod_{\alpha=1}^{N} (z_\alpha + 1)^2}. \qquad (3.36)$$

This result can be generalized to an arbitrary kernel. We get the following expression for the backscattering amplitude:

$$\begin{aligned} \gamma_C(Q) &= \frac{1}{2} \exp\left\{2 \int_{-i\infty}^{+i\infty} \frac{dz}{2\pi i} \frac{\phi'(Q; z)}{\phi(Q; z)} \ln(1 + z)\right\} \\ &= \frac{1}{2} \exp\left\{-2 \int_{-i\infty}^{+i\infty} \frac{dz}{2\pi i} \frac{\ln\phi(Q; z)}{1 + z}\right\}. \end{aligned} \qquad (3.37)$$

In the case of point scattering, we get

$$\gamma_C(Q) = \frac{1}{2} \exp\left\{-\frac{2}{\pi} \int_0^{\pi/2} d\beta \, \ln\left(1 - \frac{\arctan\sqrt{Q^2 + \tan^2\beta}}{\sqrt{Q^2 + \tan^2\beta}}\right)\right\}. \qquad (3.38)$$

For small values of the reduced wave vector Q, the result (3.38) assumes the general form (2.47), corresponding to the triangular shape of the backscattering cone. The value for $Q = 0$ reads

$$\gamma(1, 1) = \frac{[\tau_1(1)]^2}{6} = 4.227\,681\,04, \qquad (3.39)$$

in agreement with Eq. (3.32), whereas ΔQ, defined in Eq. (2.47), reads

$$\Delta Q = \frac{1}{2}, \qquad (3.40)$$

in agreement with Eq. (2.49).

D. Arbitrary albedo and n-scattering events

We conclude this section devoted to exact results by investigating briefly the situation where the albedo a of the scattering process is smaller than unity. In this case, the light intensity is partially absorbed at each scattering event. Besides its own interest, the study of this situation also allows us to determine the contribution of various scattering events to the physical quantities in the situation of elastic scattering without absorption, considered

so far ($a = 1$).

Let us consider first, for the sake of simplicity, the amplitude of the normally reflected diffuse intensity, for a normally incident beam. We have

$$\gamma(a; 1, 1) = \int_0^{\infty} \Gamma(a; \tau) \, e^{-\tau} \, d\tau, \qquad (3.41)$$

where $\Gamma(a; \tau)$ is the solution of the following Milne equation:

$$\Gamma(a; \tau) = a \, e^{-\tau} + a \int_0^{\infty} M_B(\tau, \tau') \, \Gamma(a; \tau') \, d\tau'. \qquad (3.42)$$

In this integral equation, which generalizes Eq. (2.10), the single-scattering albedo a multiplies both the source term and the kernel.

As a consequence, $\gamma(a; 1, 1)$ can be viewed as the generating function of the contributions γ_n of n-scattering events to the total amplitude $\gamma(1, 1)$ in the case of unit albedo, namely

$$\gamma(a; 1, 1) = \sum_{n \, (\geq 1)} \gamma_n a^n. \qquad (3.43)$$

Equation (3.42) can also be solved exactly by means of the approach exposed in Sec. III B. We thus obtain

$$\gamma(a;1,1) = \frac{a}{2}\exp\left[I(a)\right], \qquad (3.44)$$

with

$$I(a) = -\frac{2}{\pi}\int_0^{\pi/2} d\beta \ \ln(1 - a\beta\cot\beta) = \sum_{n\ (\geq 1)} I_n a^n, \qquad (3.45)$$

so that

$$I_n = \frac{2}{\pi n}\int_0^{\pi/2} d\beta(\beta\cot\beta)^n. \qquad (3.46)$$

The n-scattering contributions γ_n can therefore be expressed in terms of the integrals I_n, according to

$$\gamma_1 = \frac{1}{2}, \quad \gamma_2 = \frac{I_1}{2},$$
$$\gamma_3 = \frac{I_1^2}{4} + \frac{I_2}{2}, \quad \gamma_4 = \frac{I_1^3}{12} + \frac{I_1 I_2}{2} + \frac{I_3}{2}, \qquad (3.47)$$
etc.

When the number n of scattering processes becomes large, the integral formula (3.46) for the I_n is dominated by the vicinity of $\beta = 0$. We get the following power law:

$$I_n \approx \sqrt{\frac{3}{\pi n^3}} = 0.977\,205\,02 n^{-3/2}, \qquad (3.48)$$

and, by using Eq. (3.44),

$$\gamma_n \approx \gamma(1,1)\sqrt{\frac{3}{\pi n^3}} = 4.131\,311\,15 n^{-3/2}. \qquad (3.49)$$

The $n^{-3/2}$ exponent of the above laws can be shown [7] to be intimately related to the triangular shape (2.47) of the backscattering cone. Both these salient features of multiply scattering media are already described qualitatively by the diffusion approximation.

We end this section be mentioning the expression for the backscatter cone amplitude for isotropic scattering by point scatterers with an arbitrary albedo

$$\gamma_C(a;Q) = \frac{a}{2}\exp\left\{-\frac{2}{\pi}\int_0^{\pi/2} d\beta \ \ln\left(1 - a\frac{\arctan\sqrt{Q^2 + \tan^2\beta}}{\sqrt{Q^2 + \tan^2\beta}}\right)\right\}. \qquad (3.50)$$

This result shows that the backscattering amplitude is an analytic function of Q^2, as soon as the scattering albedo a is smaller than unity. This confirms the physical intuition that the triangular shape of the cone is due to the existence of arbitrarily long diffusive paths. It is therefore a characteristic of the problem with unit albedo, i.e., with no absorption, in a half-space geometry. When the reduced wave vector Q and the strength of absorption $(1 - a)$ are both small, we observe the following scaling behavior:

$$\gamma_C(a;Q) \approx \frac{\gamma_C(1;0)}{1 + 2\sqrt{Q^2 + 3(1 - a)}}. \qquad (3.51)$$

The denominator of this expression is not reproduced quantitatively by the diffusion approximation [see, e.g., Ref. [16], Eq. (71)], although it pertains to the long-distance physics of the problem. We also notice that the prefactor of the square root is nothing but the reciprocal of the value (3.40) of ΔQ.

IV. THE REGIME OF LARGE INDEX MISMATCH

The approach exposed in Sec. III has yielded a coherent derivation of many exact results in the absence of internal reflections, most of them having been known for a long time. Unfortunately, for mathematical reasons, it definitely cannot be extended to the case $n_0 \neq n_1$ where there are internal reflections. In this general situation, we have therefore to rely on either approximate or numerical methods.

In this section, we present a systematic analytical

scheme, which yields predictions concerning the behavior of physical quantities, in the regime where the optical indices n_0 and n_1 are very different from each other, i.e., when their ratio m goes to zero or infinity.

The predictions of this large-index-mismatch approach will be compared with numerical values in Sec. V. It turns out that they provide good estimates for most of the physical quantities over the whole range of values of the index ratio m. This approach is especially accurate for $m > 1$, i.e., in usual experimental situations, where the refractive index of the random medium (a liquid or a solid) is larger than that of the outside (air).

Moreover, this approach can be systematically improved in the sense that it amounts to considering only the leading term in a perturbative expansion. The first correction term will be derived explicitly in the case of the effective thickness τ_0 of the skin layer.

A. Diffuse reflection and transmission

In the extreme situations where the ratio $m = n_0/n_1$ of both optical indices is strictly zero (infinite), there is total reflection for any incidence angle for light outside the diffusive medium (inside the medium), except for the strictly normal direction. Both Milne kernels become identical in these limits. Indeed, we have $R(\mu) = 1$ for all μ, so that $M_L(\tau, 0) = M_B(\tau, 0)$.

For finite values of the ratio m, we set

$$M_L(\tau, 0) = M_B(\tau, 0) - N(\tau, 0), \qquad (4.1)$$

with

$$N(\tau,0) = \int_0^1 \frac{d\mu}{2\mu} \, T(\mu) \, e^{-\tau/\mu}. \qquad (4.2)$$

When m is very small or very large, the difference $N(\tau,0)$ is much smaller than the bulk Milne kernel $M_B(\tau,0)$. As a consequence, it is expected that the action of the kernel N can be treated somehow perturbatively.

The following point, however, makes the analysis more subtle. Equation (2.14) for the special Green's function $G_S(\tau,\tau')$ can be recast as

$$G_S(\tau,\tau') = \delta(\tau - \tau')$$
$$+ \int_0^\infty [M_B(\tau - \tau'',0) + M_B(\tau + \tau'',0)]$$
$$\times G_S(\tau'',\tau') \, d\tau''$$
$$- \int_0^\infty N(\tau + \tau'',0) \, G_S(\tau'',\tau') \, d\tau''. \qquad (4.3)$$

For $m = 0$ or $m = \infty$, the kernel $N(\tau,0)$ vanishes identically. Only the first integral thus remains in Eq. (4.3). It is easily realized that this limiting form of Eq. (4.3) only determines the Green's function up to an additive constant. This constant is determined by the action of the kernel N, and can thus be expected to diverge as $m \to 0$ or $m \to \infty$.

We are led by this observation to consider the following expansion:

$$G_S(\tau,\tau') = C_S + G_0(\tau,\tau') + G_1(\tau,\tau'), \qquad (4.4)$$

where the constant C_S diverges, whereas $G_0(\tau,\tau')$ remains finite and $G_1(\tau,\tau')$ goes to zero as $m \to 0$ or $m \to \infty$.

By inserting the expansion (4.4) into Eq. (4.3), we obtain for the finite part $G_0(\tau,\tau')$ of the Green's function the following equation:

$$G_0(\tau,\tau') = \delta(\tau - \tau')$$
$$+ \int_0^\infty [M_B(\tau - \tau'',0) + M_B(\tau + \tau'',0)]$$
$$\times G_0(\tau'',\tau') \, d\tau''$$
$$- C_S \int_0^\infty N(\tau + \tau'',0) \, d\tau'', \qquad (4.5)$$

together with a consistency condition

$$\int_0^\infty d\tau \int_0^\infty d\tau' N(\tau + \tau',0) G_0(\tau',\tau'') = 0, \qquad (4.6)$$

which expresses that the omitted contribution $G_1(\tau,\tau')$ does indeed vanish as $m \to 0$ or $m \to \infty$.

If we integrate Eq. (4.5) with respect to τ, the integrals of the finite part G_0 cancel out, and the constant C_S is determined as

$$C_S = \frac{4}{T}, \qquad (4.7)$$

where we have introduced the *mean flux transmission coefficient* T and the *mean flux reflection coefficient* $\mathcal{R}$, defined as

$$T = \int_0^1 2\mu \, T(\mu) \, d\mu, \qquad \mathcal{R} = \int_0^1 2\mu \, R(\mu) \, d\mu. \qquad (4.8)$$

These quantities obey the sum rule $T + \mathcal{R} = 1$ and depend only on the ratio m of optical indices. The mean transmission T can be evaluated exactly from the expression of the transmission amplitude $T(\mu)$ given in Table I. We thus obtain

$$T = \begin{cases} \dfrac{4m(m+2)}{3(m+1)^2} & \text{for } m \le 1 \\[2mm] \dfrac{4(2m+1)}{3m^2(m+1)^2} & \text{for } m \ge 1. \end{cases} \qquad (4.9)$$

This quantity takes, of course, its maximal value $T = 1$ for $m = 1$, around which it has the shape of an asymmetric cusp. As expected, it falls off for small and large m, according to

$$T \approx \frac{8m}{3} \quad (m \to 0), \qquad T \approx \frac{8}{3m^3} \quad (m \to \infty). \qquad (4.10)$$

The asymptotic behavior, for $m \to 0$ or $m \to \infty$, of most quantities of physical interest is immediately obtained by replacing the special Green's function $G_S(\tau,\tau')$ of the problem by the constant C_S, given by Eq. (4.7).

As far as reflection and transmission properties are concerned, we obtain the following expressions:

$$\tau_0 \approx \frac{4}{3T}, \qquad \tau_1(\mu) \approx \frac{4\mu}{T}, \qquad \gamma(\mu_a,\mu_b) \approx \frac{4\mu_a\mu_b}{T}.$$
$$(4.11)$$

As a consequence, our predictions in the $m \to \infty$ limit are as follows:

$$A^R(\theta_a,\theta_b) \approx \frac{6}{\pi m} \cos^2 \theta_a \cos \theta_b,$$
$$\frac{A^T(\theta_a,\theta_b)}{b + 2\tau_0} \approx \frac{3m^2}{\pi} \frac{\cos^2 \theta_a \cos \theta_b}{b + m^3}. \qquad (4.12)$$

It can be checked that the estimate (4.12) concerning reflection obeys the sum rule (2.27). The outcome concerning transmission shows an interesting crossover phenomenon when the optical thickness b and the index ratio m are simultaneously large. Indeed b is to be compared with the effective thickness of two skin layers, which grows as $2\tau_0 \approx m^3$.

The predictions (4.11) and (4.12) of the large mismatch approach will be compared with numerical results in Sec. V. Let us anticipate that a very satisfactory agreement will be found, for moderate values of the index ratio m, especially in the range $m > 1$ of most physical interest.

The above approach can be improved in a systematic fashion. Indeed, the expansion (4.4) shows that the leading behavior given in Eq. (4.11), which diverges as $1/T$ when $m \to 0$ or $m \to \infty$, is corrected by *finite parts*, given by the contribution of $G_0(\tau,\tau')$ to the quantities under consideration.

Let us illustrate how these corrections can be worked out, taking for the sake of simplicity the example of the solution $\Gamma_H(\tau)$ of the homogeneous Milne equation,

which is related to the Green's function $G_S(\tau, \tau')$ by Eq. (2.16), and yields in particular the effective thickness τ_0 of the skin layer. We set, in analogy with Eq. (4.4),

$$\Gamma_H(\tau) = \frac{4}{3\mathcal{T}} + \Gamma_0(\tau) + \Gamma_1(\tau). \qquad (4.13)$$

The finite part $\Gamma_0(\tau)$ has the following behavior for large τ:

$$\Gamma_0(\tau) \approx \tau + \tau_{0,0} \qquad (\tau \to \infty), \qquad (4.14)$$

so that we have, as a consequence of Eq. (2.13),

$$\tau_0 \approx \frac{4}{3\mathcal{T}} + \tau_{0,0} \qquad (4.15)$$

in the large-index-mismatch regime.

We aim at an explicit determination of the finite part $\tau_{0,0}$ of τ_0. It turns out that both situations with a large index mismatch, i.e., $m \to 0$ and $m \to \infty$, have to be dealt with in a separate way.

$m \to 0$. In this first regime, the transmission $T(\mu)$ becomes uniformly small, namely $T(\mu) \approx 3\mathcal{T}\mu/2$, so that the second integral of the rhs of Eq. (4.3) has a limit $-3E_3(\tau)$, with the definition

$$E_3(\tau) = \int_0^1 \mu \, d\mu \; e^{-\tau/\mu}. \qquad (4.16)$$

We thus have to solve the equation

$$\Gamma_0(\tau) = -E_3(\tau) + \int_0^\infty [M_B(\tau - \tau', 0) + M_B(\tau + \tau', 0)]$$
$$\times \Gamma_0(\tau') \, d\tau', \qquad (4.17)$$

with the consistency condition

$$\int_0^\infty \Gamma_0(\tau) E_3(\tau) d\tau = 0. \qquad (4.18)$$

Surprisingly enough, it turns out that the solution of Eq. (4.17) assumes exactly the linear-plus-constant form (4.14), with

$$\tau_{0,0} = -\frac{3}{4}. \qquad (4.19)$$

$m \to \infty$. In this second case, the transmission $T(\mu)$ is peaked around $\mu = 1$, so that the second integral of the rhs of Eq. (4.3) admits the limit form $-\exp(-\tau)$. We thus have to solve the equation

$$\Gamma_0(\tau) = -\frac{e^{-\tau}}{3} + \int_0^\infty [M_B(\tau - \tau', 0) + M_B(\tau + \tau', 0)]$$
$$\times \Gamma_0(\tau') \, d\tau', \qquad (4.20)$$

with the consistency condition

$$\int_0^\infty \Gamma_0(\tau) e^{-\tau} d\tau = 0. \qquad (4.21)$$

We have solved Eqs. (4.20) and (4.21) by the numerical

procedure to be exposed in Sec. V A, and obtained in particular

$$\tau_{0,0} \approx -1.0357. \qquad (4.22)$$

It is worthwhile to compare the predictions (4.19) and (4.22) with the results of the diffusion approximation. This scheme amounts to approximating the function $\Gamma_0(\tau)$ by its asymptotic linear-plus-constant form (4.14) and determining the constant $\tau_{0,0}$ by means of the consistency conditions (4.18) and (4.21). For $m \to 0$, the result (4.19) is recovered exactly. For $m \to \infty$, the diffusion approximation yields $\tau_{0,0} = -1$, which differs only by a tiny amount from the "exact" numerical value (4.22).

Another result is worth being mentioned, namely that the special solution $\Gamma_S(\mu; \tau)$ corresponding to a normally incident beam ($\mu = 1$), has a vanishing finite part in the case $m \to \infty$. This can be checked by inserting the consistency condition (4.6), with $N(\tau)$ proportional to $\exp(-\tau)$, into the definition (2.18). As a consequence, the quantities $\tau_1(1)$ and $\gamma(1, \mu_b)$ *have no finite-part correction*, so that their leading expressions (4.11) are expected to be very good as $m \to \infty$.

B. Enhanced backscattering cone

The amplitude of the backscattering cone at normal incidence can also be determined analytically, for $m \to 0$ or $m \to \infty$, in the regime where enhanced backscattering is dominated by long-distance effects, i.e., for small values of the reduced wave vector Q. For $m \ll 1$ or $m \gg 1$, and $|Q| \ll 1$, we are led to look for a solution of the form

$$\Gamma_C(Q; \tau) \approx \gamma_C(Q) \; \exp(-|Q|\tau) \qquad (4.23)$$

to the Q-dependent Milne equation (2.44), recast in the form

$$\Gamma_C(Q; \tau) = e^{-\tau} + \int_0^\infty [M_B(Q; \tau - \tau'', 0)$$
$$+ M_B(Q; \tau + \tau'', 0)]\Gamma_C(Q; \tau') \, d\tau'$$
$$- \int_0^\infty N(Q; \tau + \tau'', 0) \; \Gamma_C(Q; \tau') \, d\tau'. \qquad (4.24)$$

In analogy with the treatment of Eq. (4.3), we integrate Eq. (4.24) with respect to τ. The integral of the bulk kernel M_B is obtained by setting $s = 0$ in Eq. (3.34). Since Q is small, we expand $m(Q; 0) = (\arctan Q)/Q \approx 1 - Q^2/3$, whereas the Q dependency of the kernel N is negligible.

We thus predict the following scaling form of the cone near its top:

$$\gamma_C(Q) \approx \frac{12}{3\mathcal{T} + 4|Q|} \qquad (Q \to 0, \mathcal{T} \to 0). \qquad (4.25)$$

The result (4.25) is valid for all values of the scaling variable $Q/\mathcal{T}$. It admits the following small-Q expansion

$$\gamma_C(Q) \approx \frac{4}{T} - \frac{16|Q|}{3T^2} + \cdots. \tag{4.26}$$

The two coefficients of the result (4.26) can alternatively be obtained by inserting the expressions (4.11) into Eqs. (2.47) and (2.49).

The above formulas show in particular that the amplitude $\gamma_C(Q)$ of the backscattering cone becomes very narrow for a large index mismatch, with a reciprocal slope ΔQ and a full width at half height ΔQ_{FWHH} vanishing according to

$$\Delta Q \approx \frac{3T}{4}, \qquad \Delta Q_{\mathrm{FWHH}} \approx \frac{3T}{2}\frac{1-T/4}{1+T/4}. \tag{4.27}$$

Finally, as a consequence of the last remark of Sec. IV A, we can assert that the results (4.25)–(4.27) have *no correction of relative order* T *as* $m \to \infty$.

V. NUMERICAL RESULTS

In this section, we present numerical results concerning various physical quantities in the situation of isotropic scattering by pointlike objects in the presence of internal reflections, i.e., for arbitrary values of the ratio m of the optical indices. These predictions have been obtained by a numerical solution of the integral Milne equations, as explained below. They will be compared with the results of Sec. IV, which were established in the large-index-mismatch regime.

A. Diffuse reflection and transmission

General formulas for the diffuse reflected and transmitted intensity have been derived in Sec. II. These quantities are related, respectively, by Eqs. (2.24) and (2.34) to the functions $\Gamma_H(\tau)$ and $\Gamma_S(\mu;\tau)$, pertaining to the half-space geometry and introduced in Sec. II B.

In order to evaluate these functions numerically, it is absolutely essential to subtract their asymptotic behavior for large τ, given by Eq. (2.13). These explicit subtractions of the leading diffusive behavior allow for a very accurate numerical treatment of optically thick slabs, with an arbitrary thickness $b \gg 1$, contrarily to previous approaches [7,16]. Hence we set

$$\begin{aligned} \Gamma_H(\tau) &= \tau + \tau_0 + F_H(\tau), \\ \Gamma_S(\mu;\tau) &= \tau_1(\mu) + F_S(\mu;\tau). \end{aligned} \tag{5.1}$$

The new unknown functions $F_H(\tau)$ and $F_S(\mu;\tau)$ fall off very fast as $\tau \to \infty$, essentially as $\exp(-\tau)$. This property makes them well suited for numerical analysis. They obey the following integral equations:

$$F_H(\tau) - \int_0^\infty M(\tau,\tau')\, F_H(\tau')\, d\tau' = S_1(\tau) + \tau_0\, S_2(\tau), \tag{5.2}$$

$$F_S(\mu;\tau) - \int_0^\infty M(\tau,\tau')\, F_S(\mu;\tau')\, d\tau' \\ = e^{-\tau} + \tau_1(\mu)\, S_2(\tau),$$

where the source terms read

$$\begin{aligned} S_1(\tau) &= \frac{1}{4}\big[(1-\tau)e^{-\tau} + \tau^2 E_1(\tau)\big] \\ &\quad + \int_0^\infty M_L(\tau,\tau')\, \tau'\, d\tau', \end{aligned}$$

$$S_2(\tau) = \frac{1}{2}\big[-e^{-\tau} + \tau E_1(\tau)\big] + \int_0^\infty M_L(\tau,\tau')\, d\tau', \tag{5.3}$$

with the notation

$$E_1(\tau) = \int_0^1 e^{-\tau/\mu}\frac{d\mu}{\mu} = 2M_B(\tau,0). \tag{5.4}$$

The integral equations (5.2), with a given source term on their rhs, have been solved numerically by discretizing the functions and the kernels on the lattice of points $\{\tau_n = n\epsilon\}$ for $n = 1,\ldots,N$, i.e., $0 < \tau < \tau_{\max} \equiv N\epsilon$, and by replacing the integrals by Riemann sums. The problem is thus reduced to solving a linear system, i.e., to a numerical matrix inversion, which has been performed by using standard routines.

To be more specific, the parameter τ_0 and the function $F_H(\tau)$ have been determined by solving the first equation of (5.2), successively with the source terms $S_1(\tau)$ and $S_2(\tau)$. Let $F_1(\tau)$ and $F_2(\tau)$ be the solutions thus obtained. τ_0 is then determined by the linear condition that the combination $F_1(\tau) + \tau_0 F_2(\tau)$ falls off at infinity, i.e., practically vanishes at or near $\tau = \tau_{\max} = N\epsilon$. A similar procedure works for $\tau_1(\mu)$ and $F_S(\mu;\tau)$. We used the typical values $\epsilon = 0.05$ and $\epsilon = 0.025$, and $\tau_{\max} = N\epsilon = 10$. The numerical results were found to converge exponentially with respect to $\tau_{\max}$ and to admit a smooth linear extrapolation in ϵ.

Throughout this numerical work, we have considered, for definiteness, the following typical values of the ratio of optical indices: $m = 1/2, 2/3, 3/4, 1, 4/3, 3/2$, and 2. We have evaluated reflection and transmission properties, for a beam with unit intensity, incident from an arbitrary direction θ_a. For $m = 1$, i.e., in the absence of internal reflections, the numerical analysis reproduces very accurately the exact analytical results exposed in Sec. III.

Figures 2 and 3 show plots of the reflected and transmitted intensity, A^R and A^T for a normally incident beam ($\theta_a = 0$), against the observation angle θ_b. These quantities are maximal at normal incidence and decrease when going off the normal direction.

More precisely, for $m < 1$, the diffuse reflection and transmission vanish identically for $\sin\theta_b > 1/m$, since the incident beam undergoes total reflection, and thus does not enter the sample. In the other situation ($m > 1$), these quantities vanish linearly as grazing incidence is approached ($\theta_b \to \pi/2$) because of the explicit Fresnel transmission factor T_b in their expressions (2.24) and (2.34). Only in the absence of internal reflections do the reflection and transmission have nonzero limit values for $\theta_b = \pi/2$, which can be derived from the exact solution of Sec. III, namely
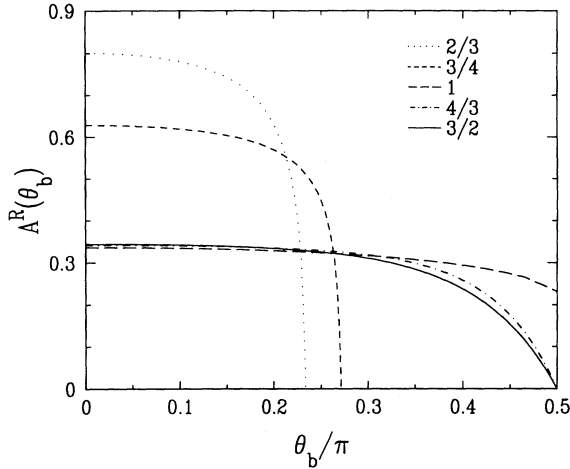
FIG. 2. Plot of the diffuse reflected intensity A^R, for a normally incident beam, against observation angle θ_b, for five values of the ratio m of optical indices.

$$A^R(0, \pi/2) = A^T(0, \pi/2) = \frac{\tau_1(1)}{4\pi\sqrt{3}} = 0.231\,396\,21$$

$$(m = 1). \quad (5.5)$$

Let us now turn to a detailed comparison between the outcomes of the large mismatch approximation of Sec. IV and numerical results. We have plotted in Fig. 4, against the ratio m of both optical indices, the following three quantities: (i) the parameter $\tau_1(1)$, defined in Eqs. (2.13) and (2.19), characterizing the diffuse transmission at normal incidence; (ii) the parameter $\gamma(1,1)$, defined in Eq. (2.25), characterizing the diffuse reflection at normal incidence; and (iii) the ratio τ_0/D, where the parameter τ_0, defined in Eq. (2.13), is a measure of the effective reduced thickness of the skin layers, and where
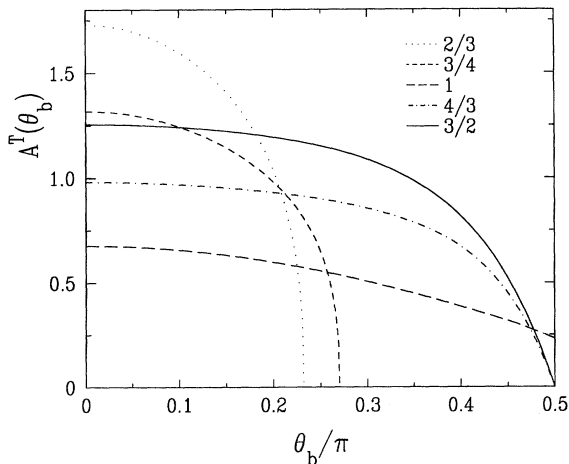

FIG. 3. Plot of the diffuse transmitted intensity A^T, for a normally incident beam, against observation angle θ_b, for five values of the ratio m of optical indices.
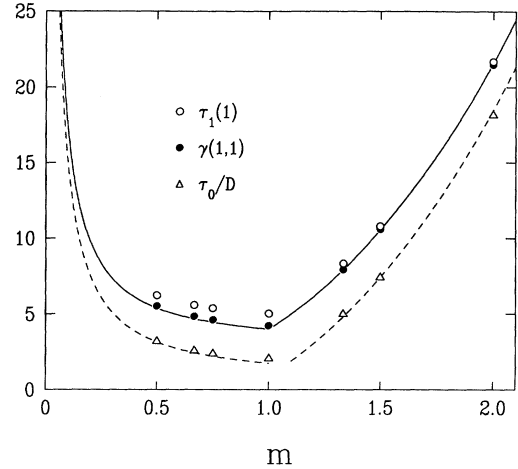

FIG. 4. Comparison between numerical results and analytic predictions of the large-index-mismatch approximation. The symbols show numerical values listed in Table II. The quantities plotted against the ratio m of optical indices, namely $\tau_1(1)$, $\gamma(1,1)$, and τ_0/D, are respectively proportional to the diffuse transmission and reflection at normal incidence, and to the effective thickness of the skin layers. The full line shows the common leading behavior of the three quantities in the large-index-mismatch regime, namely $4/\mathcal{T}$, where $\mathcal{T}$ is the mean flux transmission coefficient. The dashed lines show the improved predictions for τ_0/D, involving the finite-part corrections (4.19) and (4.22) to the leading large-index-mismatch behavior.

$D = 1/3$ is the value (2.17) of the diffusion coefficient for isotropic scattering.

According to the results (4.11), the three above quantities have the same leading behavior in the large-index-mismatch regime, i.e., for $m \to 0$ or $m \to \infty$, namely they diverge as $4/\mathcal{T}$, where is the mean flux transmission $\mathcal{T}$ has been evaluated in Eqs. (4.9) and (4.10). This asymptotic law is shown as a full line in Fig. 4 for all values of the index ratio m.

Surprisingly enough, the large-mismatch approximation provides a very satisfactory description of the dependence of physical quantities against the index ratio m, even for moderate values of this parameter, and especially in the range of physical interest ($m \geq 1$). Moreover, it is apparent in Fig. 4 that the leading discrepancy between the plotted data and the full line consists in roughly constant differences, corresponding to the finite parts discussed in Sec. IV A.

In the case of τ_0, we have obtained in Eqs. (4.19) and (4.22) the numerical values of the finite part $\tau_{0,0}$, in both regimes $m \to 0$ and $m \to \infty$. The improved predictions thus obtained are shown in Fig. 4 as two dashed lines. Including the finite-part corrections yields a spectacular improvement. This observation strengthens our confidence in the large-index-mismatch approach.

As far as $\tau_1(1)$ and $\gamma(1,1)$ are concerned, we have shown at the very end of Sec. IV A that these quantities have a vanishing finite-part correction for $m \to \infty$.

TABLE II. Numerical values of the quantities plotted on Figs. 4 and 6 for seven typical values of the ratio m of optical indices.

m	τ_0	$\tau_1(1)$	$\gamma(1,1)$	ΔQ
2	6.08	21.7	21.5	0.136
3/2	2.50	10.8	10.6	0.269
4/3	1.69	8.34	7.94	0.343
1	0.710 446	5.036 48	4.227 68	1/2
3/4	0.815	5.39	4.63	0.479
2/3	0.881	5.60	4.85	0.465
1/2	1.09	6.25	5.55	0.427

This is nicely confirmed by the fact that all data points for $m > 1$ almost lie on top of the full curve which represents the leading estimate. The data for $m < 1$ are compatible with very small finite-part corrections, which have not been evaluated numerically.

The numerical values of the quantities considered above, as well as the reciprocal slope ΔQ of the backscattering cone, are listed for completion in Table II.

B. Enhanced backscattering cone

The numerical procedure described above has been extended in order to determine the enhanced backscattering amplitude $\gamma_C(Q)$. To do so, we have discretized the Q-dependent Milne kernels $M_B(Q;\tau,\tau')$ and $M_L(Q;\tau,\tau')$ and the unknown function $\Gamma_C(Q;\tau)$ on the lattice of points $\{\tau_n = n\epsilon\}$.

We have considered the same values of the ratio m of optical indices as in Sec. V A. Figure 5 shows plots of the quantity

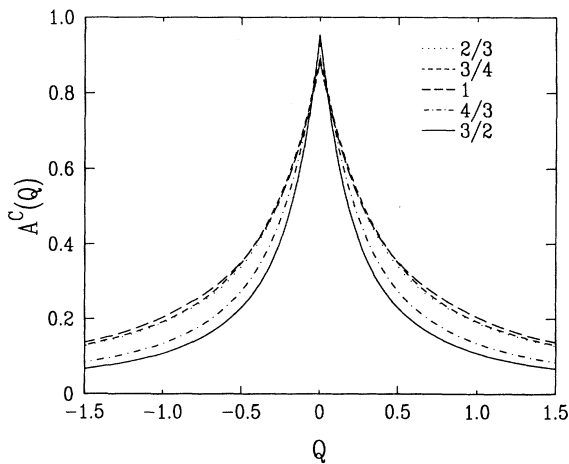$$A^C(Q) = \frac{\gamma_C(Q) - 1/2}{\gamma_C(0)}, \qquad (5.6)$$

FIG. 5. Plot of the magnitude $A^C(Q)$ of the enhanced backscattering cone, normalized with respect to the diffuse reflection, for a normally incident beam, against the reduced scattering vector $Q = k_1 l \theta_b = k_0 l \theta'_b$, for five values of the ratio m of optical indices.
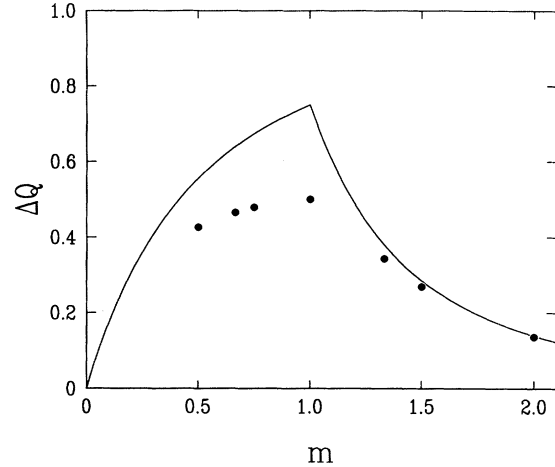

FIG. 6. Comparison between the large-index-mismatch approximation and numerical results, concerning the reciprocal slope of the enhanced backscattering cone. Symbols show numerical values plotted against the index ratio m of optical indices. The full line shows the prediction of the large-index-mismatch approach.

namely the ratio of the intensity observed in the backscattering cone to the background diffuse reflected intensity. The subtracted term $1/2$ corresponds to the contribution of single-scattering events, as explained in Sec. II E.

In order to make a comparison with the large-index-mismatch approximation, we have plotted in Fig. 6 the numerical values of the reciprocal slope ΔQ of the cone, defined in Eq. (2.47), together with the asymptotic law (4.27), shown as a full line. The vanishing of the next-to-leading correction to ΔQ, for $m \to \infty$, is again found in good agreement with numerical data. Indeed, the points for $m > 1$ are very close to the line showing the leading estimate.

VI. DISCUSSION

A. Summary

In this paper, we have studied the effects of the skin layers and especially the role of internal reflections, on the diffusive transport of light (more precisely, of scalar waves) through thick slabs of random scattering material. This analysis shows that, as long as transport is diffusive in the bulk of the medium, internal reflections lead to effects of order unity on transport properties, such as reflected and transmitted intensity, even in the limit where the mean free path is very large, as compared to the wavelength. The simple reason is that the skin layers act as barriers. The crossover from propagative to diffusive behavior, or vice versa, which takes place in the skin layers thus overshadows many higher-order interference effects ("loop diagrams"). Our work provides the basis for dealing in a systematic way with the effects of internal

reflections in skin layers. This approach yields a generalized Schwarzschild-Milne integral equation, the kernel of which has an extra contribution in the skin layers.

Among other results, we have shown in Sec. IV that most physical quantities have a leading behavior in the large-index-mismatch limit, i.e., $m \to 0$ or $m \to \infty$, that depends in a simple way on the mean flux transmission coefficient $\mathcal{T}$. We have also explained how finite-part corrections to these leading estimate can be obtained explicitly. This outcome explains to some extent the validity of a simpler approach, initiated by Lagendijk, Vreeker, and de Vries [9], according to which the effects of internal reflections are studied by means of an improved diffusion approximation. Although the effects of skin layers are, essentially by definition, beyond the scope of the diffusion approximation, such an approach works rather well in the limit of a large index mismatch, as will be discussed below. The intuitive reason for such an accord is the following. For $m \to 0$ or $m \to \infty$, the transmission at the interfaces is very small. As a consequence, because of charging effects, the effective thickness τ_0 of the skin layers becomes very large, so that the behavior of the intensity is described by a diffusion equation inside most of the skin layer, apart from a transition region of a few mean free paths.

When the index mismatch is not large, i.e., when the ratio m of both refractive indices inside and outside the scattering medium is around unity, then skin layers induce a more complex behavior of transport properties, which is described by the general formalism exposed in the present paper. Specific results concerning diffuse reflection and transmission, and the enhanced backscattering cone, have been obtained, either numerically for generic values of m (Sec. V) or exactly for $m = 1$, i.e., in the absence of internal reflections (Sec. III), where we have recovered known exact results due to astrophysicists.

Let us come back in more detail to the large-index-mismatch regime and to the improved diffusion approximation. One common step of most studies [9,22–24] consists in introducing a surface reflectivity $\mathcal{R}_S$, which represents the angular average of the ratio of the flux coming to the interface from inside the medium, to the flux reflected into the medium. In some of those works, $\mathcal{R}_S$ has not been given a quantitative definition. In Refs. [22,23], Freund and Berkovits propose a simple approach, assuming that the effects of internal reflections can be described by summing repeated partial reflections of diffuse light. Their results thus have the form of a geometric series. These cannot be quantitatively correct in the limit of large index mismatch since important simplifications occur in the outcomes of the present approach, whereas the results of these authors still involve the complicated numbers and expressions linked to the solution in the absence of internal reflections.

Some of the works quoted above can be more directly compared to ours. In Ref. [9], the estimate $\tau_0 \approx 1/\mathcal{T} - 1$ is obtained in the large-index-mismatch regime on the basis of a one-dimensional analog. This outcome differs from the correct result (4.11) by a factor of 4/3, to leading order, which represents the effect of averaging over

the beam directions. The angular dependence was then considered [25] and used as an input in numerical simulations concerning the backscattering cone for vector waves [26]. This work confirmed the narrowing of the enhanced backscattering due to internal reflections, in reasonable agreement with the results of Ref. [9].

More recently, the angular dependence has been described explicitly by Zhu, Pine, and Weitz [24]. These authors consider the case of vector waves, which can be adapted to scalar waves by neglecting the polarization dependence of the reflectivities. Consider first the regime $m \to \infty$. They introduce two coefficients, which can be estimated as

$$C_1 = \int_0^1 \mu R(\mu)\, d\mu = (1 - \mathcal{T})/2,$$

$$C_2 = \int_0^1 \mu^2 R(\mu)\, d\mu \approx 1/3 - \mathcal{T}/2,$$

(6.1)

where $\mathcal{T}$ is the mean flux transmission coefficient. In evaluating C_2 we used the fact that μ is close to unity in the $m \to \infty$ limit, unless there is total reflection. Using the identification (6.1), we find that the quantity $\mathcal{R}_S$ of Ref. [24] coincides with $\mathcal{R}$, defined in Eq. (4.8), to leading order as $m \to \infty$. As a consequence, the prediction of this article reads

$$\tau_0 = \frac{2}{3}\frac{1 + 3C_2}{1 - 2C_1} \approx \frac{4}{3\mathcal{T}} - 1. \tag{6.2}$$

This estimate compares well with (4.15) and (4.22), namely the leading term is exact and the finite part coincides with the outcome of the diffusion approximation, which only differs from the correct numerical value by a tiny amount. Let us emphasize that the determination of the constant $\tau_{0,0} = -1.0357$ requires the evaluation of the finite part G_0 of the Green's function: this task is evidently beyond the scope of diffusion approaches. Similarly, the expression given in Ref. [24] for the slope of the backscattering cone agrees, to leading order, with our prediction (4.27). This accord confirms that the use of an improved diffusion approximation makes sense to leading order in the large-index-mismatch regime.

The results of Ref. [24] can also be compared to the present ones in the $m \to 0$ limit. In this regime, C_1 is still given by Eq. (6.1), whereas we have $C_2 \approx 1/3 - 3\mathcal{T}/8$. These estimates lead to

$$\tau_0 \approx \frac{4}{3\mathcal{T}} - \frac{3}{4}, \tag{6.3}$$

in perfect agreement with (4.15) and (4.19), to the same order in $\mathcal{T}$.

B. Outlook

The present framework can be used to evaluate other quantities concerning the diffusive transport of light, such as, e.g., various speckle correlation functions. Correlations are accessible to experiment by dealing with two

different incident beams, with different angles, and/or different frequencies. The influence of internal reflections on the relative fluctuations in the angle-resolved reflected and transmitted intensities can be evaluated within the present approach. For thick slabs ($b \gg \tau_0$) and fixed incident and outgoing directions, the speckle correlation functions will exhibit the same dependence with respect to the index ratio m as the average reflection and transmission considered in this work. This matter will be the subject of a separate publication.

Our approach can be extended to the regime of moderate disorder, where $k_0 l$ is not very large. The first step of that analysis consists in investigating the microscopic scattering mechanism. This has been done recently in the case of resonant point scatterers [27]. The next step is a self-consistent treatment of the transport equation to first order in the density n of scatterers. In the bulk of the medium, this procedure will only modify numerical values, such as, e.g., that of the diffusion coefficient. In the skin layers, however, the t matrix and the mean free path will depend on the spatial position. This new effect yields a smearing of the mirror charges, which are point-like in the present work, thus making the analysis more intricate. The present approach can also be extended to the case of a stratified medium, where the density $n(z)$ of scatterers varies continuously near the air-medium interface. If the variations of $n(z)$ are smooth at the scale of the mean free path, effects similar to the smearing of mirror charges will take place. It is worth mentioning that the spatial dependence of the t matrix becomes essential in narrow geometries, such as films or waveguides.

It has been shown recently [28] that drastic interference effects take place when a new transport channel, i.e., a new cavity mode, is opened.

The case of vector waves can also be dealt with along the lines of the present work. In the regime considered here ($k_0 l \gg 1$), the propagation between scatterers will involve on-shell transversal photons. However, for a moderate disorder, the near-field longitudinal component of the electromagnetic field will also contribute to transport. This also makes the analysis more difficult. This effect has been studied in the similar situation of resonant atoms [29]. The methods developed here also apply to many other domains of physics, as testified by the example, treated in Sec. II D, of the boundary resistance of electrical contacts.

ACKNOWLEDGMENTS

[1] S. Chandrasekhar, *Radiative Transfer* (Dover, New York, 1960).

[2] A. Ishimaru, *Wave Propagation and Scattering in Random Media* (Academic, New York, 1978), Vols. 1 and 2.

[3] M.P. van Albada, B.A. van Tiggelen, A. Lagendijk, and A. Tip, Phys. Rev. Lett. **66**, 3132 (1991).

[4] A.Z. Genack, in *Scattering and Localization of Classical Waves in Random Media*, edited by P. Sheng (World Scientific, Singapore, 1990).

[5] M.P. van Albada, J.F. de Boer, and A. Lagendijk, Phys. Rev. Lett. **64**, 2787 (1990).

[6] A.Z. Genack and J.M. Drake, Europhys. Lett. **11**, 331 (1990).

[7] M.B. van der Mark, Ph.D. thesis, University of Amsterdam, 1990 (unpublished).

[8] P.N. den Outer, Th.M. Nieuwenhuizen, and A. Lagendijk, J. Opt. Soc. Am. (to be published).

[9] A. Lagendijk, R. Vreeker, and P. de Vries, Phys. Lett. A **136**, 81 (1989).

[10] H.C. van de Hulst, *Multiple Light Scattering* (Academic, New York, 1980), Vols. 1 and 2.

[11] G.D. Mahan, *Many-Particle Physics* (Plenum, New York, 1981).

[12] D.S. Fisher and P.A. Lee, Phys. Rev. B **23**, 6851 (1981).

[13] N.F. Mott and E.A. Davis, *Electronic Processes in Non-Crystalline Materials*, 2nd ed. (Clarendon, Oxford, 1979).

[14] M.P. van Albada and A. Lagendijk, Phys. Rev. Lett. **55**, 2692 (1985).

[15] P.E. Wolf and G. Maret, Phys. Rev. Lett. **55**, 2696 (1985).

[16] M.B. van der Mark, M.P. van Albada, and A. Lagendijk, Phys. Rev. B **37**, 3575 (1988).

[17] E. Akkermans, P.E. Wolf, and R. Maynard, Phys. Rev. Lett. **56**, 1471 (1986); E. Akkermans, P.E. Wolf, R. Maynard, and G. Maret, J. Phys. (Paris) **49**, 77 (1988).

[18] B.A. van Tiggelen, A. Lagendijk, and A. Tip, J. Phys. Condens. Matter **2**, 7653 (1990).

[19] B.A. van Tiggelen, Ph.D. thesis, University of Amsterdam, 1992 (unpublished).

[20] E.E. Gorodnichev, S.L. Dudarev, and D.B. Rogozkin, Phys. Lett. A **144**, 48 (1990).

[21] H.C. van de Hulst and R. Stark, Astron. Astrophys. **235**, 511 (1990).

[22] I. Freund and R. Berkovits, Phys. Rev. B **41**, 496 (1990).

[23] I. Freund, Phys. Rev. A **45**, 8854 (1992).

[24] J.X. Zhu, D.J. Pine, and D.A. Weitz, Phys. Rev. A **44**, 3948 (1991).

[25] A. Lagendijk (unpublished).

[26] R. Eisma, University of Amsterdam Report LaPdV1, 1989 (unpublished).

[27] Th.M. Nieuwenhuizen, A. Lagendijk, and B.A. van Tiggelen, Phys. Lett A **169**, 191 (1992).

[28] Th.M. Nieuwenhuizen, University of Amsterdam Report No. Nie1, 1992 (unpublished).

[29] Th.M. Nieuwenhuizen, A.L. Burin, Yu. Kagan, and G.V. Shlyapnikov, Phys. Lett. A (to be published).